# Templating of carbon in zeolites under pressure: Synthesis of pelletized zeolite templated carbons with improved porosity and packing density for superior gas ($CO_2$ and $H_2$) uptake properties

Norah Balahmar, Alexander M. Lowbridge and Robert Mokaya*

University of Nottingham, University Park, Nottingham NG7 2RD, U. K.

*E-mail: r.mokaya@nottingham.ac.uk (R. Mokaya)*

## Abstract

This report explores the use of compacted zeolite pellets as templates for the preparation of pelletized zeolite templated carbons (ZTCs). The effects of zeolite compaction before use as hard templates were investigated through the compression of powder forms of zeolites at 370 MPa or 740 MPa prior to their use as templates. The resulting carbon samples were compared to compacted conventionally templated (with powdered zeolites) ZTC. The use of compacted zeolite pellets results in pelletized ZTCs that simultaneously exhibit higher porosity and higher packing density, which translates to highly enhanced volumetric gas ($CO_2$ and hydrogen) uptake. For CVD-derived samples, the pelletized ZTCs achieve 10% higher surface area than powdered samples (and reach > 2000 $m^2$ $g^{-1}$) despite their packing density increasing from ca. 0.55 to 0.85 g $cm^{-3}$, which means that the surface area per unit volume increases by ca. 60% from between 1000 and 1100 $m^2$ $cm^{-3}$ for the powdered ZTCs to ca. 1670 $m^2$ $cm^{-3}$ for pelletized samples. Thus their volumetric $CO_2$ uptake at 25 $^oC$ increases by 140% and 85% at 1 and 20 bar, respectively, compared to powdered ZTCs. Pelletized ZTCs prepared via a combination of liquid impregnation and CVD achieve much higher surface area of 3000 $m^2$ $g^{-1}$ (compared to 2700 $m^2$ $g^{-1}$ for powder samples) despite an increase in packing density from 0.44 to 0.69 g $cm^{-3}$, resulting in a surface area per unit volume rise of 75% from 1189 $m^2$ $cm^{-3}$ to 2085 $m^2$ $cm^{-3}$. The high surface area pelletized ZTCs have attractive gravimetric hydrogen uptake of 6.6 wt% (5.5 wt% for powdered sample) at 20 bar and -196 $^oC$, and reach volumetric hydrogen storage capacity of 46 g $l^{-1}$ (24 g $l^{-1}$ for powder sample). For $CO_2$ uptake at 25 $^oC$ and at 20 bar, the volumetric uptake of the high surface area pelletized ZTC is nearly twice that of the powdered sample; 668 g $l^{-1}$ compared to 360 g $l^{-1}$.

## 1. Introduction

Porous materials have been extensively investigated as storage media for energy related gases such as hydrogen and $CO_2$. The focus on porous materials as stores for energy applications is driven and motivated by the need for environmental protection and demands for clean energy sources.[1,2] The drive for environmental protection is typified by research efforts aimed at developing materials for the capture and sequestration of $CO_2$, while the search for cleaner energy sources requires material advances that may lead to realisation of the mooted Hydrogen Economy.[1-19] Innovative synthesis methods and the development of new types of nanoporous materials that offer improvements in overall porosity or high level control of porosity have brought significant strides in addressing the materials challenges that must be overcome in the journey towards materials-based $CO_2$ storage and the Hydrogen Economy.[3-8,20]Thus porous materials with very high surface area and/or well controlled porosity have recently come on to the research stage. The best examples of such research are illustrated by developments in metal organic frameworks (MOFs),[21] covalent organic frameworks (COFs)[22] and porous carbons whether they be activated[4] or templated.[5,23-25] Given the relationship between porosity and gas uptake, improvements in surface area and pore volume, and better targeting of pore size has resulted in materials with attractive gravimetric uptake for $CO_2$ and hydrogen;[3-8,26,27] the gas uptake capacity of porous materials under any given conditions generally strongly correlates with the magnitude of the surface area and size of pore channels.[3-8,26,27] Due to their more robust stability under various environments, porous carbons have retained on-going interest as gas stores even on the face of other emerging materials such as MOFs and COFs.[4,5,23-25] Of particular interest are zeolite templated carbons, which, so far, not only exhibit some of the highest reported surface area values for carbons but also offer enhanced pore size control due to the templating effect of zeolite frameworks.[24,28-31]

Material-based developments in the storage of $CO_2$ and hydrogen are generally guided by set targets that would allow practical use of the materials in a commercially viable manner. Examples of such targets include those of the United States Department of Energy (DOE) which, for hydrogen storage, currently stipulate a whole system uptake of 5.5 wt% (gravimetric) and 40 g $l^{-1}$ (volumetric), with the ultimate aim being a gravimetric uptake of 7.5 wt% and volumetric capacity of 70 g $l^{-1}$.[32] Therefore, there is need to not only increase the gravimetric uptake of porous materials but even more importantly, to improve the volumetric storage capacity. Recent trends in the development of porous materials for $CO_2$ and hydrogen storage have mainly emphasised porosity changes that allow improvements in the gravimetric uptake.[3-19] This has included preparation of ultra-high surface area nanostructures for gas uptake at high pressures,[21,22] and on the other hand, synthesis of highly microporous materials for $CO_2$ uptake at low pressure.[7,33-39] Unfortunately, at the present time, the materials with the highest surface area generally tend to have low packing density and therefore low volumetric uptake. Enhancements in packing density and consequently volumetric storage capacity of porous materials may be achieved by material densification or compaction. However, for most porous materials, attempts at densification generally fail to achieve the desired outcome due to the fact that increase in packing density causes a decrease in porosity due to the inherent mechanical instability of most nanostructures. Densification via compaction, therefore, generally results in drastic decrease in both the porosity (surface area and pore volume) and gravimetric uptake of $CO_2$ and hydrogen. In this regard, whilst porous carbons are generally mechanically robust and can withstand moderate densification, MOFs and COFs on the other hand, have low mechanical stability and are easily destroyed with loss of porosity even at low compaction pressures.[40-43]

Examples of porous solids with varying mechanical stability and amenability to compaction include; activated carbons compacted at 40 MPa that reach a packing density of 0.5 g $cm^{-3}$ and hydrogen storage capacity of 20 g $l^{-1}$ (at -196 $^{o}$C and 40 bar),[40,41] monolithic forms of activated

carbon with packing density of 0.7 g $cm^{-3}$ that achieve a total volumetric hydrogen uptake capacity of 39 g $l^{-1}$ at -196 $^{o}$C and 44 bar,[44] compacted activated carbon with a packing density of 0.72 g $cm^{-3}$ with volumetric hydrogen uptake capacity of 41 g $l^{-1}$ at -196 $^{o}$C and 60 bar.[45] More recently, we have shown that so-called compactivated carbons, which are prepared via a mechanochemical approach involving compaction of carbonaceous matter before activation, show improvements in porosity and may be densified to higher packing density than conventionally activated carbons, and therefore show attractive volumetric gas ($CO_2$ and Hydrogen) uptake.[46] On the other hand, compaction of MOFs yields less promising results; compaction of a MOF-5, achieves an uptake of ca. 16 g $l^{-1}$ (at -196 $^{o}$C and pressure of between 40 and 60 bar).[45,47] Other examples of MOF densification include those of; (i) Chahine and co-workers (38 and 48 g $l^{-1}$ at 50 and 130 bar, respectively, and -196 $^{o}$C for densified MOF-177),[48] (ii) Muller and co-workers (38 and 48 g $l^{-1}$ at 50 and 80 bar, respectively, and -196 $^{o}$C for densified MOF-5),[49] Siegel and co-workers (38 and 43 g $l^{-1}$, respectively, at 50 and 100 bar and -196 $^{o}$C for densified MOF-5).[50] Much less work has been reported on the effects of densification of porous materials on their volumetric $CO_2$ uptake; Marco-Lozar and co-workers have reported on activated carbon monoliths that have high packing density and volumetric $CO_2$ uptake,[51] while we have achieved improvements in volumetric uptake of activated carbons via a mechanochemical activation (so-called compactivation) route.[52]

Zeolites, which are known to have high mechanical stability, have in the recent past been extensively studied for carbon templating, as they offer a wide range of porous structures for carbon materials to adopt with a high level of structural ordering.[23,24] Zeolite-templated carbons (ZTCs) are prepared by the carbonisation of a zeolite, in which a carbon precursor fills the zeolite's porous framework to adopt its reciprocal structure.[24] Following the removal of the zeolite template via selective etching, the resulting carbon structure exhibits a network of pore channels that are inversely replicated from the zeolite. Past efforts to increase the volumetric gas uptake of ZTCs

include the densification of zeolite Y-templated carbon by Kyotani and co-workers via hot-pressing at 300 $^{o}$C and 147 MPa, which achieved packing density of between 0.7 and 0.9 g $cm^{-3}$.[53] More recently, we have shown that ZTCs have excellent mechanical stability and are amenable to densification to packing density of ca. 0.72 g $cm^{-3}$ and consequently a rise in volumetric hydrogen storage capacity from 30 g $l^{-1}$ to values greater than 50 g $l^{-1}$ at 20 bar and -196 $^{o}$C.[54] However, despite the excellent mechanical stability of the ZTCs, there was a loss of porosity on compaction.[54] It is therefore of interest to explore other possible densification routes for this robust group of templated porous carbons. Motivated by the known high mechanical stability of zeolites, we herein explore the effect of templating ZTCs from compacted zeolite pellets. This is the first time that compacted zeolites, in the form of pellets, have been used as templates for nanostructured carbon, and represents an entirely new approach to the synthesis of ZTCs. An added attraction of this new approach is that, importantly, it has the potential to generate densified ZTCs. We report on the properties of compacted pelletized zeolite templated carbons generated from zeolites pressed into pellets at high pressure and the consequences of such compaction on porosity, densification and both gravimetric and volumetric gas (hydrogen and $CO_2$) uptake.

## 2. Experimental section

### *2.1. Material synthesis*

To test the full range of applicability of the proposed synthesis route, we prepared ZTCs via two synthesis regimes that generate carbons with either moderate or high surface area.

**I. Moderate surface area ZTCs**

Conventionally templated (i.e., powder) ZTCs were prepared as follows; 0.5 g of dry zeolite (13X or Y) was heated at a ramp rate of 10 $^{o}$C $min^{-1}$ to 700 °C under nitrogen. Chemical vapour deposition was then performed for 3 h at 700 $^{o}$C with a flow of nitrogen saturated with acetonitrile, following

which the gas flow was switched to nitrogen only and the temperature increased at a ramp rate of 10 $^{o}$C min$^{-1}$ to 900 °C and held for 3 h, followed by cooling to room temperature under nitrogen. The resulting zeolite/carbon composite was treated sequentially in 10% hydrofluoric acid at room temperature, washed in distilled water and then refluxed (at 60 $^{o}$C) in concentrated hydrochloric acid. The final carbon was then repeatedly washed with distilled water and dried at 60 °C for 12 h to yield ca. 0.1 g ZTC, denoted as CZ13X or CZY for templating with zeolite 13X or zeolite Y, respectively. To probe the effects of post-synthesis compaction, ca. 40 mg of both CZ13X and CZY were compacted into pellets at a load of 5 tonnes on a 1.3 cm diameter die, equivalent to 370 MPa of compaction pressure; the compacted samples were denoted as C5-CZ13X and C5-CZY, respectively.

To explore the effects of templating with compacted zeolite pellets, 0.5 g Zeolite 13X or 0.23 g of Zeolite Y was compacted into a pellet at a load of 5 tonnes on a 1.3 cm diameter die, equivalent to 370 MPa of compaction pressure. The compaction increased the zeolite density by nearly 50% from 0.7 g cm$^{-3}$ to 1.08 g cm$^{-3}$. The carbon templating process was carried out as described above for powder samples except that the resulting zeolite/carbon composites were placed in HF and HCl acids as described above but *with no agitation* so as to preserve a compact pelletized nature. The washing cycle was repeated until the zeolite framework was etched out, and the final carbons, denoted as CZ13XP and CZYP from zeolite 13X and zeolite Y, respectively, were washed with deionised water and dried at 60 $^{o}$C. The yield of carbon for the pelletized ZTCs was similar to that of the conventionally templated powder samples.

**II. High surface area ZTCs**

High surface area ZTCs were prepared as follows; 0.6 g zeolite 13X (powder or compacted into a pellet at 10 tonnes equivalent to 740 MPa) was dried in a furnace at 300 °C for 12 h before being

impregnated, via the incipient wetness method, with furfural alcohol (FA). The resulting FA/zeolite composite, in an alumina boat, was heated under argon flow at 80 °C for 24 h followed by further heating at 150 °C for 8 h. The temperature was then raised at a ramp rate of 5 $^{o}$C min$^{-1}$ to 700 °C and held for 3 h under argon flow. The resulting zeolite/carbon composite was then exposed to further carbon deposition via CVD with ethylene gas (10% in argon by volume) at 700 °C for 3 h. The gas flow was then switched to argon only and the temperature raised to 900 °C and held for 3 h followed by cooling under argon to room temperature. The resulting zeolite/carbon composites were washed in 10% HF for 24 h and then refluxed in concentrated HCl for 6 h. No stirring was applied during washing of the compact pelletized sample. The final carbon material, denoted as CZ13XFAET (powder) or CZ13XFAETP (compacted pellets) was washed with deionised water and dried at 100 °C for 24 h.

### *2.2. Materials characterisation*

Powder XRD analysis was performed on either a Bruker D8 Advance powder diffractometer or a PANalytical X'Pert PRO diffractometer using CuKα radiation and operating at 40 kV and 40 mA, with 0.02$^{o}$ step size and 2 to 30 s step time. Thermogravimetric analysis was carried out in alumina pans using a TA Instruments SDT Q600 analyser with heating rate of 10 $^{o}$C min$^{-1}$ to 1000 $^{o}$C under flowing (100 mL min$^{-1}$) air conditions. Prior to porosity analysis, the carbons were dried in an oven and then degassed overnight at 200 ˚C under vacuum. The textural properties were determined by nitrogen sorption at -196 $^{o}$C using a Micromeritics ASAP 2020 volumetric sorptometer. The surface area was calculated by using the BET method applied to adsorption data in the relative pressure (P/Po) range of 0.06 – 0.22. The total pore volume was determined from the amount of nitrogen adsorbed at P/Po = 0.99. Micropore surface area and micropore volume were obtained via *t*-plot analysis. The pore size distribution was determined by a non-local density functional theory

(NLDFT) method using nitrogen adsorption data. Scanning electron microscopy (SEM) images were obtained using an FEI Quanta 650 ESEM or JEOL 6490LV instrument. Transmission electron microscopy (TEM) images were obtained using a JEOL 2100 FEG-TEM instrument. Raman spectra were recorded using a Horiba LabRAM Raman microscope.

### *2.3. Gas uptake measurements*

$CO_2$ uptake measurements were performed on a Hiden intelligent gravimetric analyzer (IGA-003), which has a pressure range of 0 – 20 bar. Before analysis, the carbon samples were outgassed overnight under vacuum at 250 $^oC$. Then the $CO_2$ uptake isotherms were obtained at 0 $^oC$ and 25 $^oC$ in the pressure range 0 – 20 bar. Hydrogen uptake measurements were performed using high-purity hydrogen (99.9999%) additionally purified by a molecular sieve filter over the pressure range of 0 – 20 bar with a Hiden intelligent gravimetric analyzer (IGA-003). Prior to analysis, the samples were dried in an oven for 24 h at 80 $^oC$ overnight and then placed in the analysis chamber and degassed at 200 $^oC$ and $10^{-10}$ bar for 4 – 6 h. Then the hydrogen uptake isotherms were measured at -196 $^oC$ (under a liquid nitrogen bath). The hydrogen uptake was corrected for buoyancy effect as previously described.[29,30] The hydrogen uptake was calculated based on skeletal density of 1.5 g $cm^{-3}$ for the carbons, which was obtained was determined from helium sorption data obtained using the IGA at a pressure of up to 20 bar at 0 $^oC$.

## 3. Results and discussion

Prior to their use as templates, we ascertained the nature of compacted zeolites with respect to their morphology, structural ordering and porosity. We thus compared samples of zeolite 13X compacted at 5 tonnes (370 MPa) or 10 tonnes (740 MPa) with original powder samples. SEM images (Supporting Figure S1, S2 and S3) show that whilst powder samples of zeolite 13X have well

dispersed and ‘free flowing’ standalone particles (Figure S1), compaction causes aggregation of the particles, and that the extent of aggregation increases at higher compaction pressure (Figure S2 and S3). Individual zeolite particles are still observed in the compacted zeolites but mainly as part of larger aggregates. The compaction, clearly, leads to a decrease in interparticle voids, which manifest in the form of higher packing density as mentioned above. However, the compaction and change in packing density does not have any significant effect of the structural ordering of the zeolite as shown by XRD patterns (Figure S4). The XRD patterns of the powder and compacted (at 10 tonnes) zeolite samples are similar, which confirms the mechanically robust nature of the zeolites. Furthermore the porosity of the zeolites remains largely unchanged after compaction according to nitrogen porosity analysis (Figure S5). The nitrogen sorption isotherms and pore size distribution curves (Figure S5) are similar for powder and compacted zeolites. The textural properties and pore size of the zeolites remain unchanged by the compaction (Table S1).

### *3.1 Zeolite templated carbons prepared via CVD*

We have previously shown that powder forms of zeolite 13X and zeolite Y may be used as templates for the formation of ZTCs with moderate surface area via a chemical vapour deposition route.[55,56] In the present study we used powder zeolites as control (baseline) experiments. To confirm that the compacted zeolite pellets generated purely carbonaceous ZTCs, we performed thermogravimetric analysis (TGA). Figure 1 shows TGA curves of zeolite Y, pelletized zeolite Y/carbon composite and the final pelletized ZTC (CZYP). The air dried zeolite Y shows a mass loss of ca. 20 wt% up to 300 °C due to loss of of water, and thereafter remains thermally stable up to 1000 °C. The zeolite/carbon composite shows a mass loss of ca. 30 wt% between 450 and 630 $^{o}$C, which is attributable to the combustion of the carbon component.[55,56] The pelletized CZYP carbon shows one main mass loss event due to carbon burn off, which commences at ca. 440 $^{o}$C and is complete at 630 $^{o}$C. The TGA

curve for the CZYP carbon shows that the pelletized ZTC is virtually zeolite-free, with a residual mass typically less than 1 wt% at 1000 °C. Thus the use of compacted zeolite pellets as template offers no major variation in terms of carbon yield, thermal stability and etching of the zeolite framework.

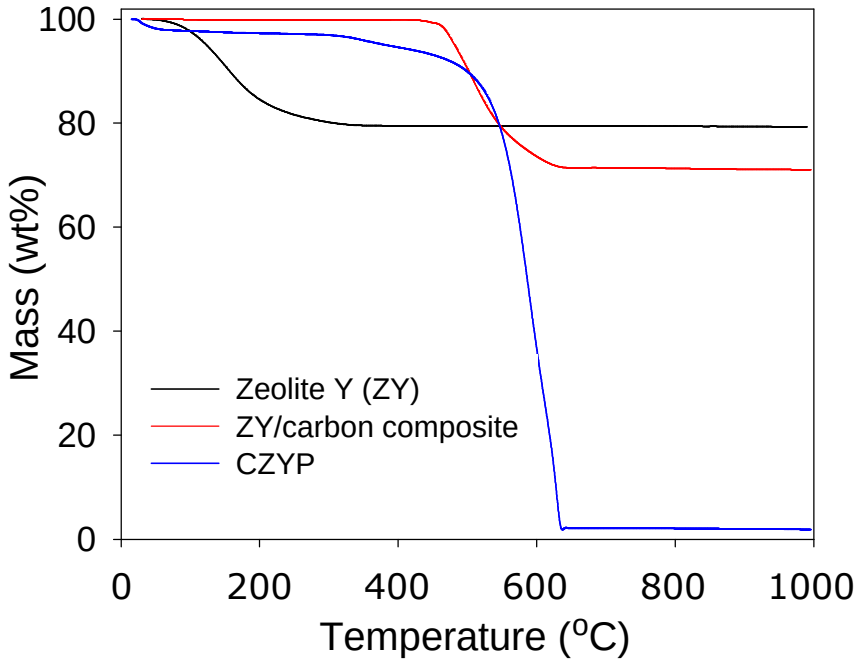


**Figure 1**. Thermogravimetric analysis curves of zeolite Y, zeolite Y/carbon composite and carbon CZYP.

A main motivation of the present work is to increase the packing density of the final ZTCs. We have recently shown that the packing density of ZTCs may be increased by direct compaction of the carbons.[54] In the present study, it is the zeolite that is compacted prior to use as a template for the formation of ZTCs. As mentioned above, the packing density of the zeolite templates increased by ca. 50% from 0.7 g $cm^{-3}$ to 1.08 g $cm^{-3}$. The increase in zeolite packing density arises from compaction into smaller volume and the removal of any large interparticle voids. We ascertained

that the overall surface area and pore volume of the zeolite remained unaffected by the compaction. It is expected that the use of such compacted zeolites should yield pelletized forms of ZTCs that replicate the lack of large interparticle voids from the zeolite, with the overall effect being an increase in packing density. To retain pellet forms of ZTC, the steps involving washing of the zeolite/carbon composites in acid (HF and HCl) were performed without any agitation. However, in order to allow analysis, we loosely broke up the pellet forms of ZTCs that emerged from the compacted zeolite pellets. It emerged straight away, as shown in Figure 2A, that the ZTCs derived from compacted zeolites had a significantly higher packing density and were much less fluffy. Figure 2B shows equivalent amounts with respect to mass (i.e., 0.1 g) of CZ13XP and CZ13X. Figure 2A indicates that the pelletized CZ13XP sample is less fluffy and more compact, which is confirmed in Figure 2B where it occupies about half the volume of the powder CZ13X sample. The packing density values determined for the CVD-derived ZTCs (following a gentle compaction at load of 74 MPa),[54] are given in Table 1. The packing density of the ZTC derived from zeolite 13X increases from 0.53 g $cm^{-3}$ for powdered zeolite templating (CZ13X) to 0.82 g $cm^{-3}$ for the carbon from the compacted zeolite template (CZ13XP), which is an increase of ca. 55%. A similar increase was observed for the ZTCs derived from zeolite Y, i.e., from 0.55 g $cm^{-3}$ for CZY to 0.88 g $cm^{-3}$ for CZYP, a rise in packing density of ca. 60%. It is noteworthy that the packing density of the powdered ZTCs could also be increased by direct compaction at 370 MPa to 0.65 g $cm^{-3}$ (C5-CZ13X) and 0.71 g $cm^{-3}$ (C5-CZY). However, these packing density values are still somewhat lower than those of analogous ZTCs derived from compacted zeolite pellets.

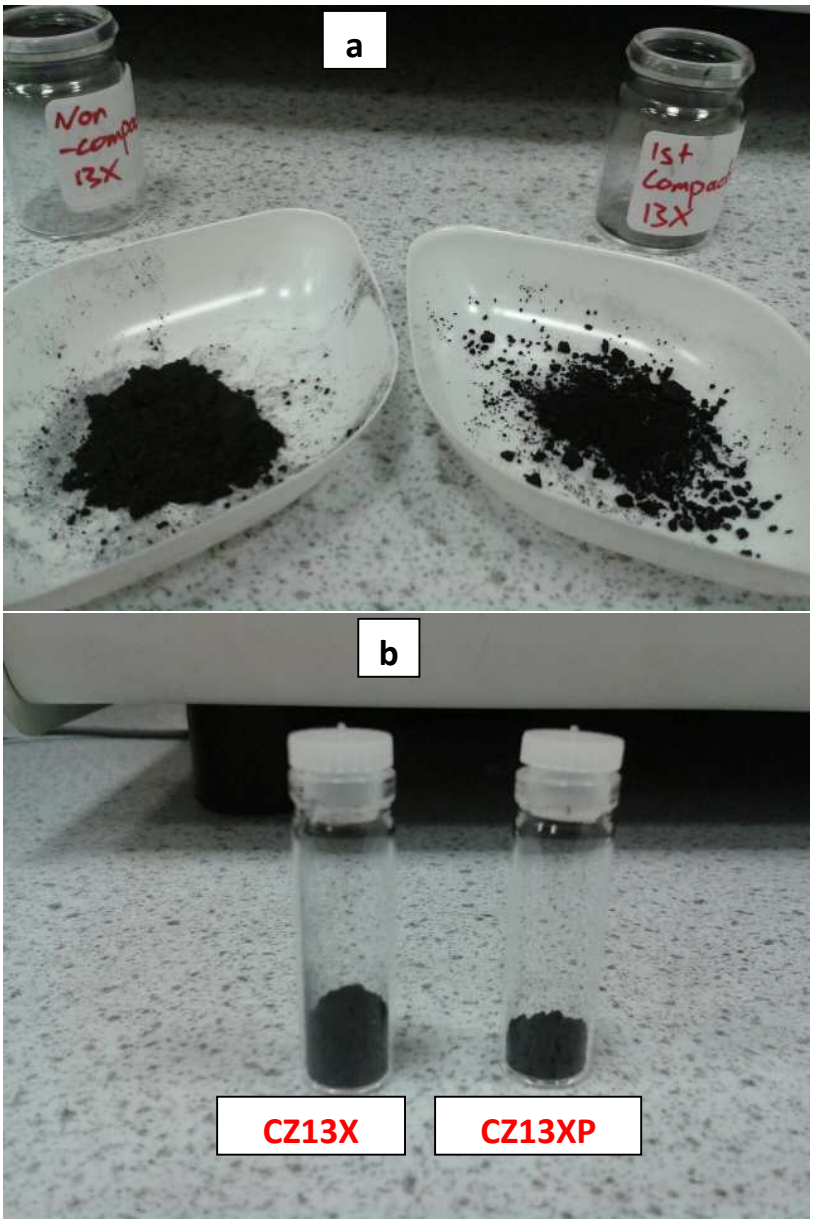


**Figure 2**. Photographic images (a) and (b) of CVD-derived ZTCs templated by powdered zeolite 13X (CZ13X) and compacted (at 370 MPa) zeolite 13X pellet (CZ13XP). The images in (b) show equal (0.1 g) amounts of ZTC and illustrate differences in packing density.

**Table 1**. Packing density, textural properties and $CO_2$ uptake of CVD-derived zeolite templated carbons templated by powdered or compacted pellets of zeolite 13X or zeolite Y.

| Sample | Packing density ($g\ cm^{-3}$) | Surface area[a] ($m^2\ g^{-1}$) | Pore volume[b] ($cm^3\ g^{-1}$) | Pore size[c] (Å) | V/S[d] $m^2\ cm^{-3}$ | $CO_2$ uptake[e] (mmol $g^{-1}$)[f] | |
|---|---|---|---|---|---|---|---|
| | | | | | | 1 bar | 20 bar |
| CZ13X | 0.53 | 1927 (1140) | 1.19 (0.53) | 7.5/12/24 | 1021 | 1.9 (44) | 11.6 (271) |
| CZ13XP | 0.82 | 2038 (1601) | 1.22 (0.75) | 7.5/12/24 | 1671 | 2.8 (101) | 13.1 (473) |
| C5-CZ13X | 0.65 | 1578 (1197) | 0.92 (0.56) | 7.5/12/24 | 1026 | 1.9 (54) | 11.6 (332) |
| CZY | 0.58 | 1654 (1143) | 0.95 (0.53) | 8/11.5/24 | 959 | 1.6 (41) | 11.2 (286) |
| CZYP | 0.88 | 1897 (1413) | 1.29 (0.66) | 8/11.5/24 | 1670 | 2.5 (97) | 13.7 (531) |
| C5-CZY | 0.71 | 1575 (1275) | 0.89 (0.60) | 8/11.5/24 | 1118 | 1.6 (50) | 11.3 (353) |

The values in the parenthesis refer to: [a]micropore surface area and [b]micropore volume. [c]pore size distribution maxima obtained from NLDFT analysis. [d]surface area per unit volume. [e]$CO_2$ uptake at 25 $^oC$ and various pressures (i.e., 1 bar and 20 bar). [f]The values in parenthesis are volumetric $CO_2$ uptake in $g\ l^{-1}$.

Figure 3 shows the nitrogen sorption isotherms of the CVD-derived ZTCs templated by powder or compacted pellets forms of zeolite 13X or zeolite Y. In each case, we also show the nitrogen sorption isotherm of the equivalent directly compacted ZTC. In all cases, the isotherms are Type I, as the nitrogen uptake is highest at low relative pressures (P/Po < 0.1), which is typical for carbons that adopt the structural ordering of zeolites.[55,56] The shape of the isotherm for the pelletized ZTC samples (CZ13XP and CZYP) is identical to that of the powder analogues (CZ13X and CZY) except that the pelletized samples have higher nitrogen sorption. A higher nitrogen sorption hints at enhancement of porosity in the pelletized ZTCs. Such an enhancement is particularly clear for CZYP compared to CZY (Figure 2C). It is also clear, based on the amount of nitrogen sorbed that in both cases, direct compaction (samples C5-CZ13X and C5-CZY) leads to a decrease in porosity.

This would suggest an advantage of the use of compacted zeolite pellets as templates over direct compaction of already prepared ZTCs with respect to retention of high porosity.

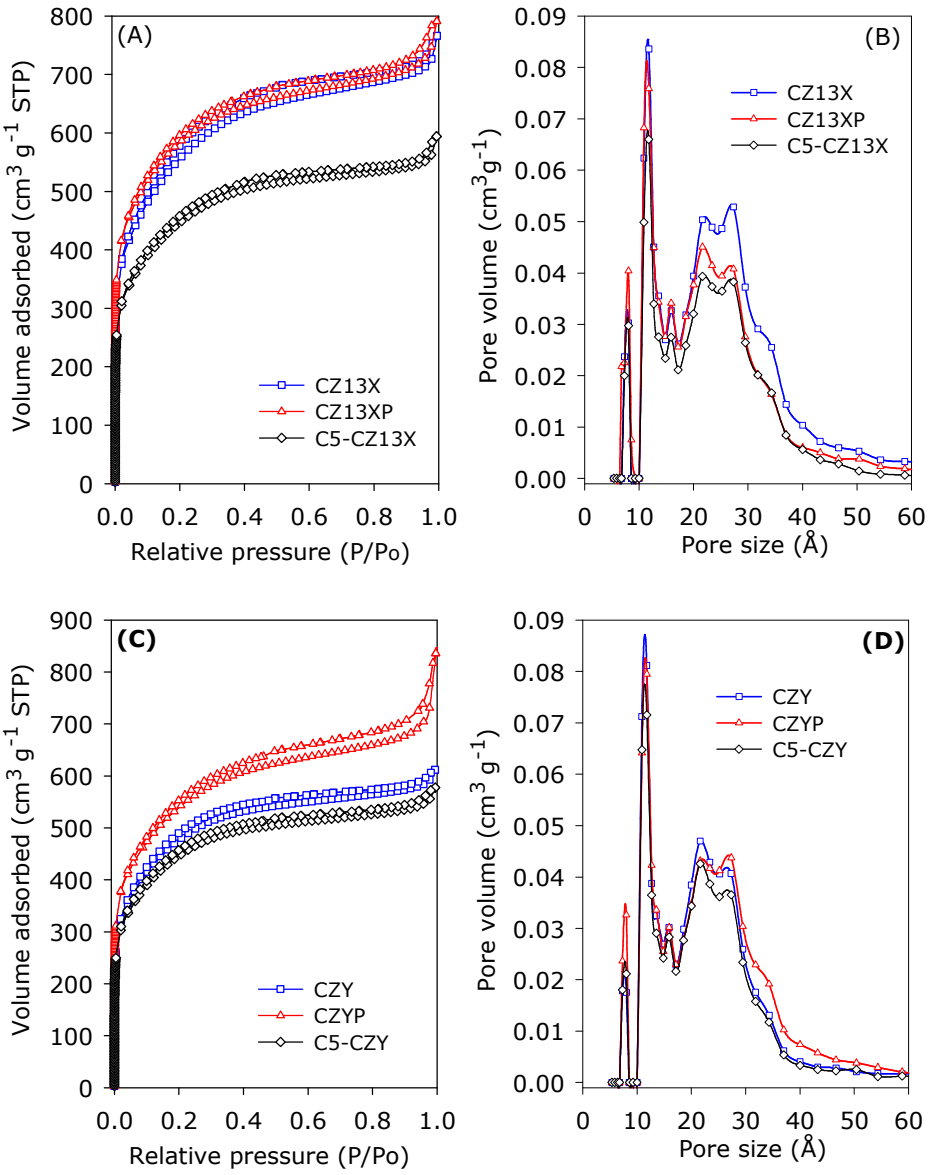


**Figure 3**. Nitrogen sorption isotherms (A, C) and corresponding pore size distribution (PSD) curves (B, D) of CVD-derived zeolite templated carbons templated by powder or compacted pellets of zeolite 13X (A, B) or zeolite Y (C, D). The nitrogen sorption isotherm and PSD curve of the equivalent directly (i.e., post-templating) compacted ZTC (C5-CZ13X and C5-CZY) is shown for comparison purposes.

The textural parameters of the CVD-derived ZTCs are summarised in Table 1. It is noteworthy that despite their higher packing density, the surface area of pelletized ZTCs templated by compacted zeolite pellets is still comparable or higher than that of analogous conventional powder samples. The surface area of CZ13X is 1927 $m^2$ $g^{-1}$ compared to 2038 $m^2$ $g^{-1}$ for the pelletized CZ13XP sample, while for zeolite Y templated carbons the pelletized CZYP sample has a significantly higher surface area (1897 $m^2$ $g^{-1}$) compared to 1654 $m^2$ $g^{-1}$ for the analogous powder ZTC (CZY). The micropore surface area of the pelletized ZTCs is between 25 and 40% higher than that of powder samples. Furthermore, both the total and micropore surface area of pelletized ZTCs is much higher than that of directly compacted C5-ZTC samples. Similar trends in pore volume are observed with the pelletized ZTCs exhibiting higher total and micropore volume (Table 1). The proportion of micropore surface area increased from ca. 60% for powder samples to 75 – 80% for the pelletized ZTCs. The improvement in both the packing density and porosity for the pelletized ZTCs means that the surface area per unit volume increased by ca. 60% from between 1000 and 1100 $m^2$ $cm^{-3}$ for the powder and directly compacted ZTCs to ca. 1670 $m^2$ $cm^{-3}$ for pelletized samples (Table 1). The PSD curves in Figure 3 (and Supporting Figure S6 and S7), and pore size data in Table 1 indicate that use of a compacted zeolite pellets as templates has little effect on the pore size.

We explored the $CO_2$ uptake properties of the CVD-derived carbons in an effort to illustrate the benefits that may arise from the higher packing density of the pelletized ZTCs. The $CO_2$ uptake was determined at 25 $^oC$ and the pressure range 0 – 20 bar. Figure 4 compares the $CO_2$ uptake isotherms of ZTCs prepared from compacted zeolites (CZ13XP and CZYP) to analogous samples that were directly compacted (C5-CZ13X and C5-CZY). We note that direct compaction did not affect the gravimetric $CO_2$ storage capacity under our measurement conditions. The $CO_2$ uptake at 1 and 20 bar is summarized in Table 1. The $CO_2$ uptake of the pelletized ZTCP carbons is at all

pressures higher than that of equivalent powder samples whether compacted or not. At 1 bar, the $CO_2$ uptake of sample CZ13XP is 2.8 mmol $g^{-1}$ compared to 1.9 mmol $g^{-1}$ for CZ13X and C5-CZ13X, which represents a nearly 50% enhancement in storage capacity for the pelletized ZTCP sample. For the zeolite Y templated carbons the $CO_2$ uptake of the ZTCP sample (CZYP) is 56% higher at 2.6 mmol $g^{-1}$ compared to 1.6 mmol $g^{-1}$ for the powdered (CZY) and directly compacted (C5-CZY) samples. A similar trend is observed at 20 bar where the $CO_2$ uptake of the pelletized ZTCP samples is between 15 and 20% higher than that of analogous powdered or directly compacted samples. We ascribe the enhancement in $CO_2$ uptake for the pelletized ZTC samples at 1 bar to their higher levels of micropore surface area. For example, the micropore surface area of pelletized CZ13XP is 1601 $m^2$ $g^{-1}$ compared to 1140 $m^2$ $g^{-1}$ for the powdered CZ13X sample, or 1197 $m^2$ $g^{-1}$ for the compacted C5-CZ13X sample. Additionally, the micropore surface area as a proportion of the total surface area is 79% for pelletized CZ13XP compared to 59% for the powdered CZ13X sample. Likewise, for pelletized CZYP, the micropore surface area is higher at 1413 $m^2$ $g^{-1}$ compared to 1143 $m^2$ $g^{-1}$ for the powdered CZY sample, or 1275 $m^2$ $g^{-1}$ for the analogous compacted C5-CZY sample. Additionally, the micropore surface area as a proportion of the total surface area is 75% for pelletized CZYP compared to 69% for the powdered CZY sample. This finding is consistent with the fact that the $CO_2$ uptake at low pressure (1 bar) is very dependent on the pore size of the carbons.[33-39] On the other hand, the greater $CO_2$ uptake of the pelletized samples at 20 bar may be ascribed to their higher overall surface area and pore volume. It is known that the $CO_2$ uptake of porous carbons at high pressure (such as 20 bar) is determined by the total surface area.[33-39]

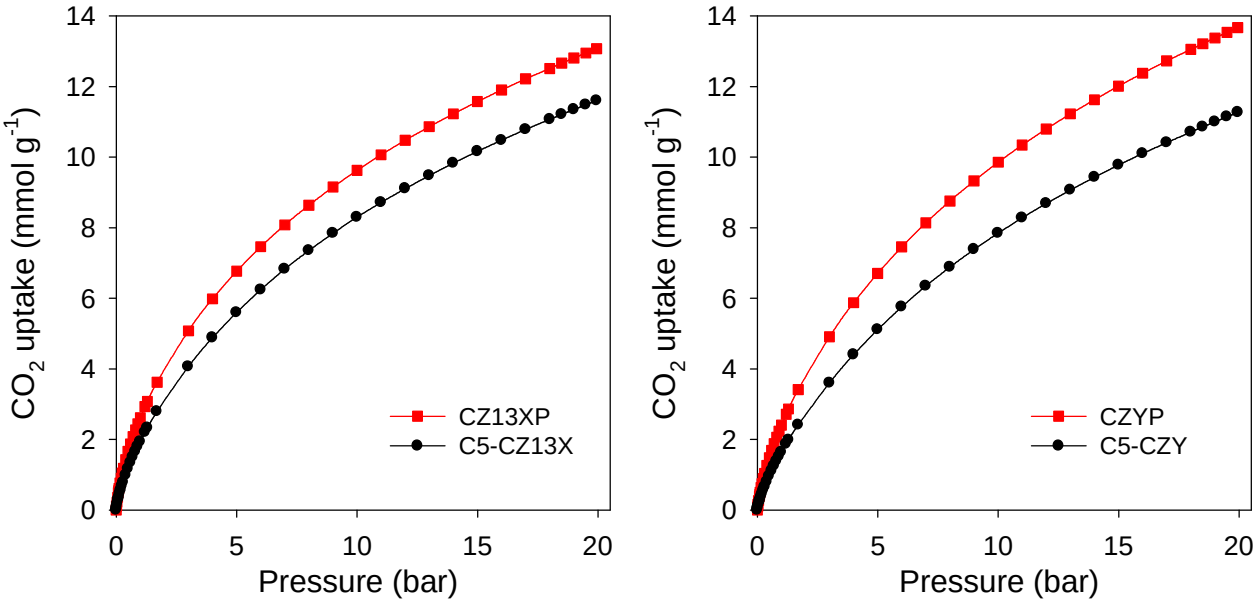


**Figure 4**. $CO_2$ uptake isotherms at 25 $^oC$ and 0 - 20 bar for variously prepared zeolite templated carbons; CZ13XP and CZYP were templated by compacted zeolite pellets, while C5-CZ13X and C5-CZY are directly compacted forms of conventionally synthesised powder samples.

Thus, purely on the basis of gravimetric $CO_2$ uptake, the porosity enhancements derived from templating with compacted zeolite pellets are evident. However, of greater significance is the improvement in volumetric $CO_2$ uptake as shown in Table 1 and Figure 5, arising from the higher packing density of the pelletized ZTCs. At 1 bar, the volumetric $CO_2$ uptake of sample CZ13XP is 101 g $l^{-1}$, which is 130% higher than 44 g $l^{-1}$ for the powder CZ13X sample, and 87% higher than 54 g $l^{-1}$ for the directly compacted C5-CZ13X carbon. For the ZTCs templated by zeolite Y, the volumetric $CO_2$ uptake of the pelletized ZTCP sample (CZYP) is 97 g $l^{-1}$, which is 137% higher than that of CZY (41 g $l^{-1}$), and nearly double that of the directly compacted C5-CZY sample (50 g $l^{-1}$). The low pressure volumetric $CO_2$ uptake enhancements of between 85 and 140% arise from the higher micropore surface area of the pelletized ZTCP samples and their greater packing density. A similar trend is observed at 20 bar although the enhancements in volumetric $CO_2$ uptake are lower at

between 40 and 85%. It is noteworthy that a volumetric uptake of up to 531 g $l^{-1}$ is achieved for sample CZYP at 20 bar and 25 $^{o}$C (Figure 5).

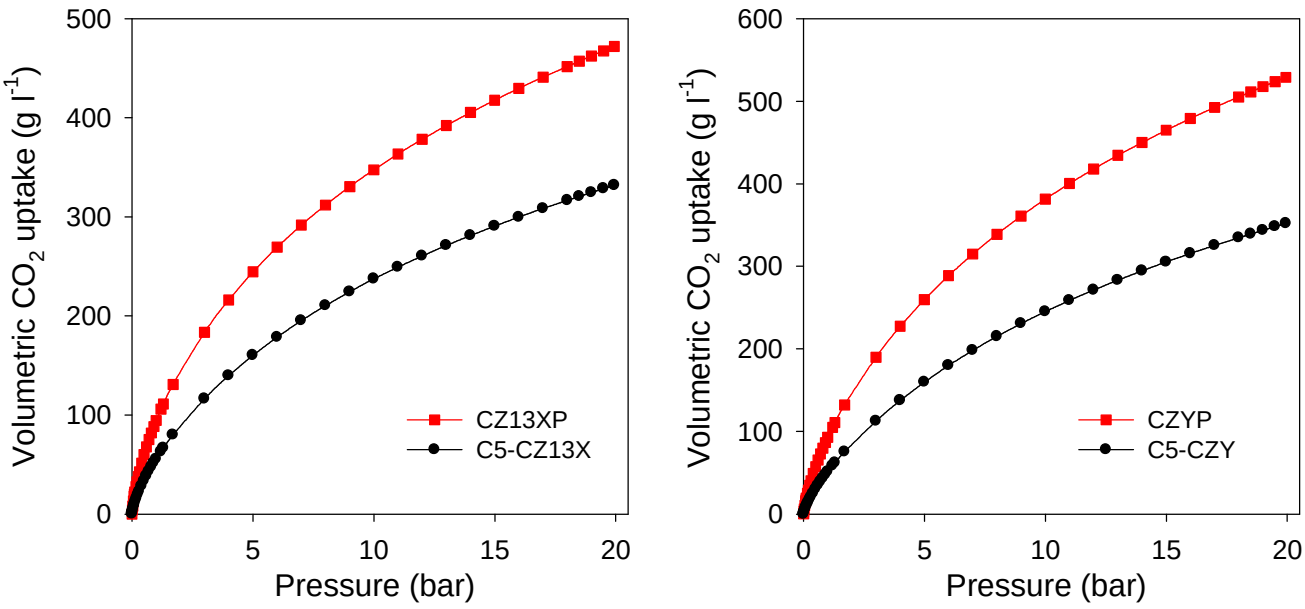


**Figure 5**. Volumetric $CO_2$ uptake at 25 $^{o}$C and 0 - 20 bar for various zeolite templated carbons; CZ13XP and CZYP were templated by compacted zeolite pellets, while C5-CZ13X and C5-CZY are directly compacted forms of conventionally synthesised powder samples.

### *3.2 Zeolite templated carbons prepared via combination of liquid impregnation and CVD*

Zeolite templated carbons with high surface area may be prepared via a synthesis route that combines liquid impregnation (LI) of a carbon precursor and CVD.[18,23,30,31,54] In order to fully explore our 'templating under pressure route' we extended the use of compacted zeolite pellets as templates to the synthesis of ZTC via both LI and CVD. We first confirmed that fully carbonaceous ZTC carbons were generated from both powder (sample CZ13XFAET) and compacted (CZ13XFAETP) zeolites (Supporting Figure S8). According to thermogravimetric analysis (Supporting Figure S8) both the pelletized (CZ13XFAETP) and powder (CZ13XFAET) ZTCs are very dry and show no mass loss below 300 $^{o}$C. At higher temperature (400 $^{o}$C - 600 $^{o}$C), both ZTCs

show a sharp mass loss due to carbon burn-off. The sharp mass loss due to carbon burn off suggests that the templated carbons are mainly one phase materials, which is an indication that the carbonaceous matter of the ZTCs is formed within the zeolite pore channels rather than both within the pores and outside as the latter carbon would be graphitic and thus have a higher burn-off temperature. The ZTCs show virtually no residual mass after 800 °C, confirming that they are zeolite free. The use of compacted zeolite 13X pellets as template for the LI + CVD nanocasting route does not appear to have any effect on the thermal properties of the ZTCs. The nature of carbon was confirmed by powder XRD patterns shown in Figure 6. The XRD pattern of the pelletized CZ13XFAETP carbon exhibits a sharp peak at 2θ = 7°, which is similar to that present in zeolite 13X (Figure 6). The peak suggest a d-spacing of ca. 1.4 nm, which is comparable to that of zeolite 13X, and indicates microporous *structural* ordering replicated from the zeolite template.[18,23,30,31,54] The XRD patterns also shows very broad features at 2θ = 25º and 44°, which, if they were sharp would be (002) and (101) diffractions from graphitic carbon. The broad nature of these features confirms that the carbon is amorphous in nature – a finding which is consistent with the carbon being formed (templated) within the zeolite pore channels; given the narrow pores of zeolite 13X, it is impossible to form stacking structures within the pores and therefore the expectation is that the resultant carbon will comprise a single graphene sheet without any stacking and are thus be largely non-graphitic.[57,58] This view is with the Raman spectra of the templated carbons (Figure S9). The carbons exhibit bands at ca. 1344 $cm^{-1}$ and 1595 $cm^{-1}$ that are, respectively, the so-called D-peak (disordered carbon) and the G-peak (graphitic domains). The ratio of peak area of the D-peak to G-peak ($I_D/I_G$), based on the two-band fitting model is 0.83 for the conventional powdered CZ13XFAET sample and 0.87 for the pelletized CZ13XFAETP carbon. The $I_D/I_G$ ratio is in a range expected for non-graphitic carbon, and also confirms that pelletization does not affect the level of graphitisation in the templated carbons. The absence of graphitisation means it is instead likely that

single nanographene-like sheets are formed in the zeolite 13X pores, curved with a bucky bowl resemblance to replicate the inner-cavities of the spherical pores of the zeolite framework.[57] The presence of sharp peaks in the pattern of the zeolite/carbon composite (Figure 6) is evidence that the zeolite framework is not destroyed and its structural ordering is not altered during the templating process despite a priori compaction of the zeolite at 740 MPa. The filling of the carbon into the zeolite pores reduces phase contrast scattering resulting in some zeolite peaks being lost or reduced in intensity in the XRD pattern of the composite.

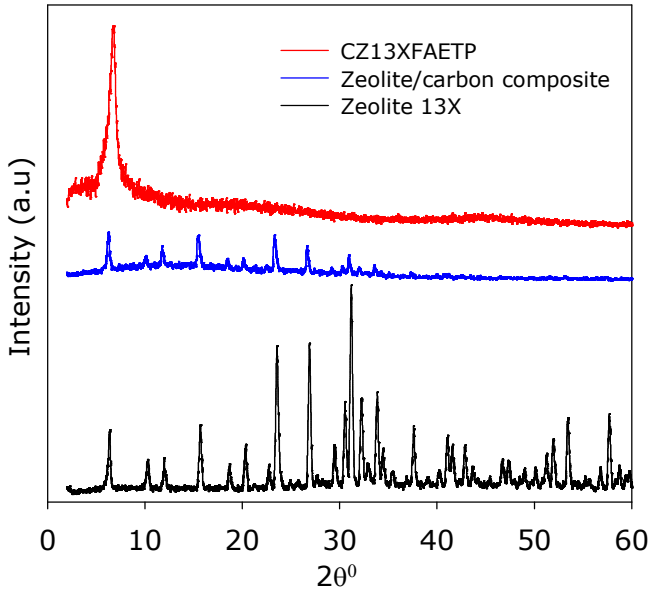


**Figure 6**. Powder XRD patterns of zeolite 13X, zeolite 13X/carbon composite and the final CZ13XFAETP carbon.

The replication process was explored by observing SEM images of the powder (CZ13XFAET) and pelletized (CZ13XFAETP) samples. In both cases (Figure 7), the morphology of the templated carbons is similar to that of the zeolite particles shown in Figure S1 and S2. The morphology of the zeolite 13X template, whether in powder or pellet form, was evidently replicated in the carbons materials, which is necessary for a templating process wherein the carbon precursor must be

transformed into a carbon framework within the zeolite pore channels. It is also clear that the individual particle size of the carbons is similar to that of the zeolite, an observation that precludes excessive deposition of carbon on the external surface of zeolites. It is noteworthy that the aggregated particles of the compacted zeolite (Figure S2) are replicated in the pelletized CZ13XFAETP sample (Figure 7 and Figure S10). This is consistent with the increase in packing density observed not only for the compacted zeolite 13X but also the pelletized zeolite templated carbon. We also confirmed that zeolite structural ordering was replicated in the templated carbons as shown by the TEM images in Figure 8. A high level of structural ordering is observed for both the powder (CZ13XFAET) and pelletized (CZ13XFAETP) ZTCs. The TEM images indicate a pore channel size of 10 – 15 Å, which is in agreement with porosity studies discussed below. The TEM images also show that there is a minor amount of graphitic/turbostratic carbon deposited as thin layers on the surface of the carbon particles but that the bulk of the carbons are amorphous as per their XRD patterns (Figure 6). Pelletization does not, therefore, have any significant effects on both the morphology and structural ordering of the ZTCs.

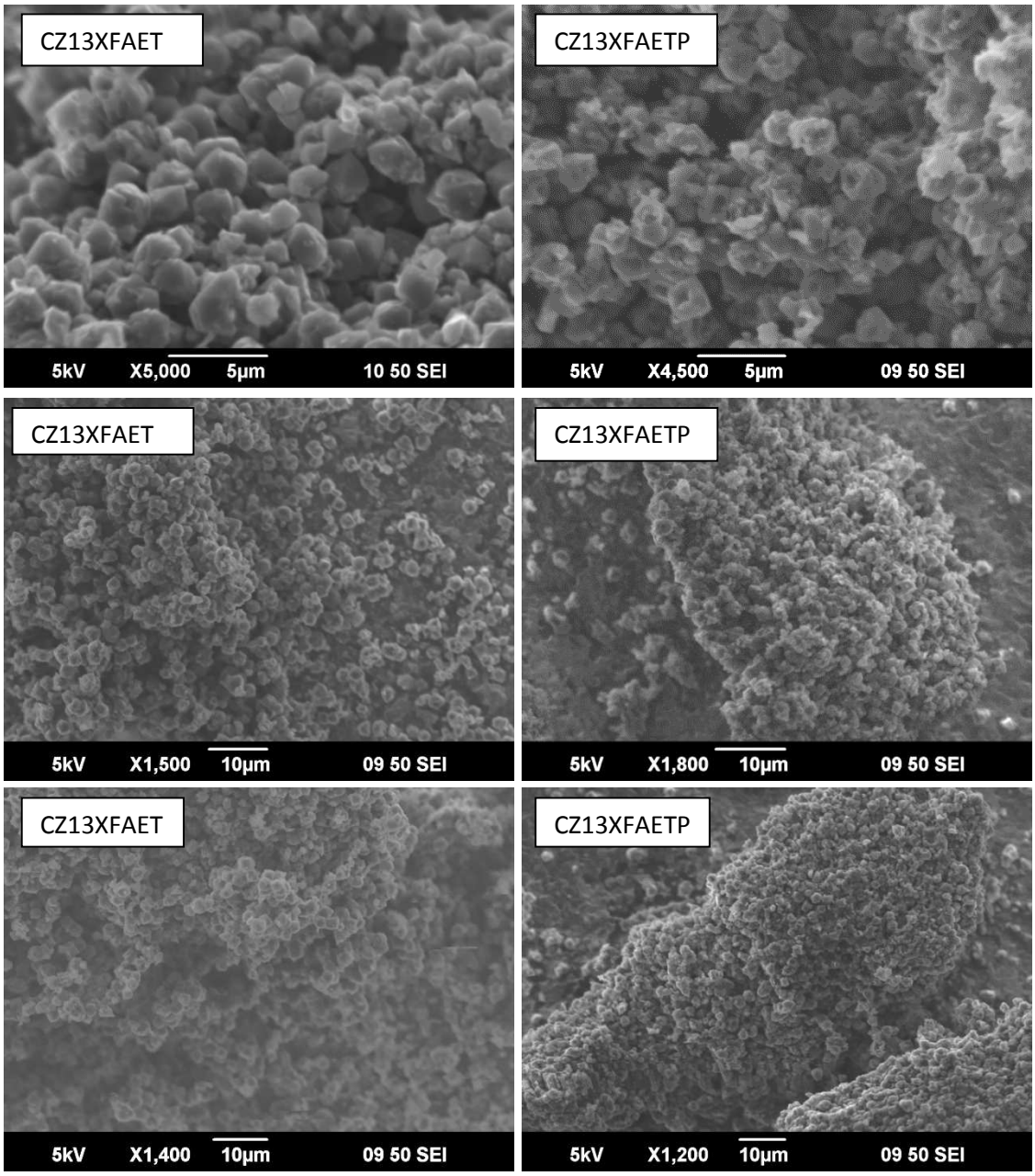


**Figure 7**. Representative SEM images of zeolite templated carbons templated by powder (CZ13XFAET) or compacted pellets (CZ13XFAETP) of zeolite 13X.

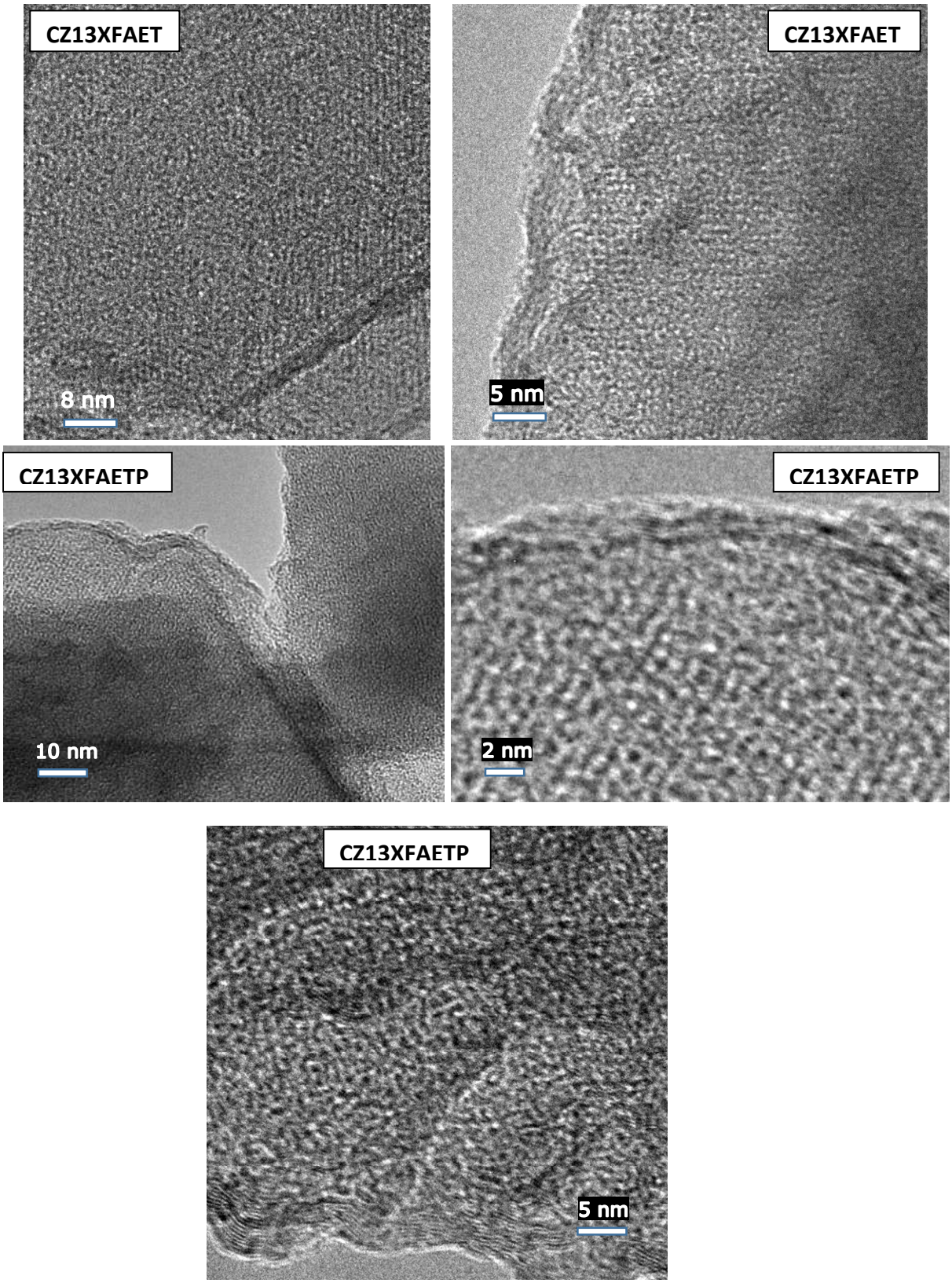


**Figure 8**. Representative TEM images of zeolite templated carbons templated by powder (CZ13XFAET) or compacted pellets (CZ13XFAETP) of zeolite 13X.

The nitrogen sorption isotherms for the pelletized and powder ZTCs are shown in Figure 9A. Both sorption isotherms are mainly type I, with a high nitrogen uptake in the low relative pressure ($P/Po \leq 0.1$) region. It is however clear that the pelletized sample has higher nitrogen sorption due to enhanced porosity. The textural properties of the ZTCs are summarized in Table 2. The powder (CZ13XFAET) ZTC has total surface area of 2702 $m^2 g^{-1}$ and micropore area of 2342 $m^2 g^{-1}$, which is typical of well-ordered zeolite templated carbons.[18,23,30,31,54] The pelletized sample (CZ13XFAETP), on the other hand, has total surface area of 3021 $m^2 g^{-1}$ and micropore area of 2448 $m^2 g^{-1}$. Thus compaction of the zeolite prior to use as template engenders a 12% increase in total surface area, while the micropore surface area shows a more modest rise of 5%. PSD curves of the two high surface area ZTCs are presented in Figure 9B (and Supporting Figure S11), and the pore size maxima values are summarised in Table 2. The average pore width of the ZTCs is 12 Å, along with a minor distribution of smaller pores at 7.5 Å. The pore channels are smaller and more sharply distributed than those of the CVD-derived ZTCs (Table 1), which suggest a high level of zeolite-like structural ordering.[18,23,30,31,59,60] Compaction of the zeolite prior to use as a template, therefore, has no effect on the PSD, similar to what is observed for CVD-derived ZTCs as discussed above. The high surface area and pore volume of the pelletized CZ13XFAETP sample is very attractive given that it has a packing density of 0.69 g $cm^{-3}$ compared to 0.44 g $cm^{-3}$ for the conventionally templated CZ13XFAET sample, which is an increase in packing density of ca. 57%. This means that the surface area per unit volume rises by 75% from 1189 $m^2 cm^{-3}$ for powdered CZ13XFAET to 2085 $m^2 cm^{-3}$ for the pelletized CZ13XFAETP sample.

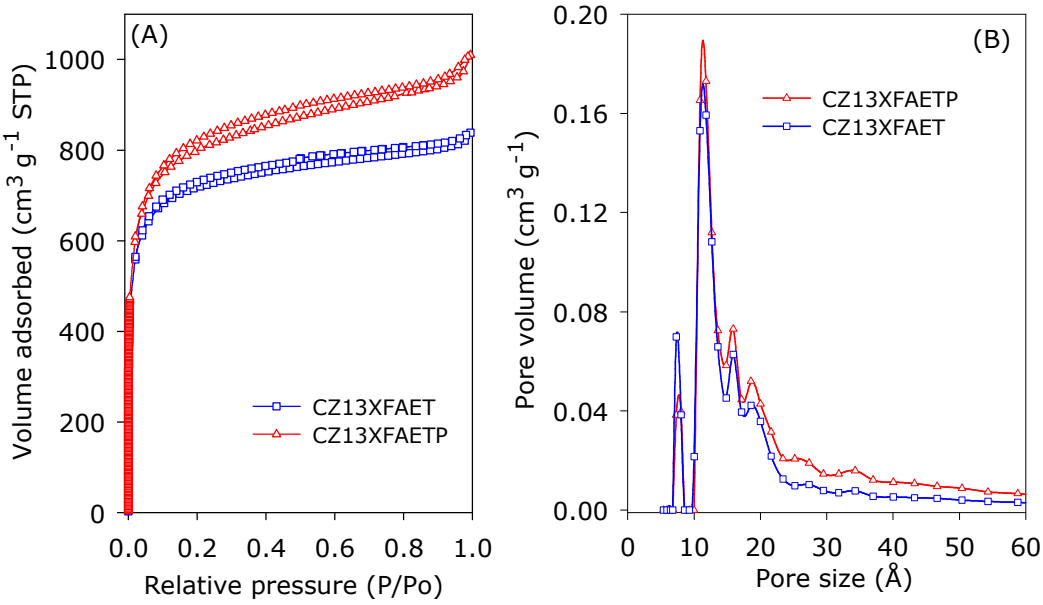


**Figure 9**. Nitrogen sorption isotherms (A) and corresponding pore size distribution (PSD) curves (B) of zeolite templated carbons templated by powder (CZ13XFAET) or compacted pellets (CZ13XFAETP) of zeolite 13X.

**Table 2**. Textural properties and gas ($CO_2$ and hydrogen) uptake of zeolite templated carbons templated by powder or compacted pellets of zeolite 13X.

| Sample | Surface area[a] ($m^2\ g^{-1}$) | Pore volume[b] ($cm^3\ g^{-1}$) | Pore size[c] (Å) | $CO_2$ uptake[d] (mmol $g^{-1}$) | | $H_2$ uptake[e] | |
|---|---|---|---|---|---|---|---|
| | | | | 1 bar | 20 bar | (wt%) | (g $l^{-1}$) |
| CZ13XFAET | 2702 (2341) | 1.30 (0.95) | 7.5/12 | 2.5 (48) | 18.6 (360) | 5.5 (4.7) | 24 (21) |
| CZ13XFAETP | 3021 (2448) | 1.56 (1.00) | 7.5/12 | 2.6 (79) | 22.0 (668) | 6.6 (5.5) | 46 (38) |

The values in the parenthesis refer to: [a]micropore surface area and [b]micropore volume. [c]pore size distribution maxima obtained from NLDFT analysis. [d]$CO_2$ uptake at 25 °C and various pressures (i.e., 1 bar and 20 bar); the values in parenthesis are volumetric $CO_2$ uptake in g $l^{-1}$. [e]Gravimetic (wt%) and volumetric (g $l^{-1}$) $H_2$ uptake at -196 °C and 20 bar; the values in parenthesis are excess $H_2$ uptake.

Given the high surface area of the ZTCs prepared via the LI + CVD route, we assessed their gas uptake for both hydrogen and $CO_2$. The total and excess hydrogen uptake isotherms of the powder and pelletized ZTCs are shown in Figure 10, and the storage capacity at 20 bar (and -196 $^oC$) is stated in Table 2. At a pressure of 20 bar, the pelletized ZTC (CZ13XFAETP) has total hydrogen uptake capacity of 6.6 wt% compared to 5.5 wt% for the powder CZ13XFAET sample. The excess hydrogen uptake at 20 bar follows a similar trend; 5.5 wt% for CZ13XFAETP and 4.7 wt% for CZ13XFAET. The gravimetric hydrogen uptake values are as expected for high surface area zeolite-templated carbons.[28,30,54] The motivation for this work was to generate materials with a high volumetric gas uptake. Figure 10B shows both the excess and total volumetric hydrogen uptake calculated on the basis of a packing/bulk density of 0.44 g $cm^{-3}$ for CZ13XFAET and 0.69 g $cm^{-3}$ for CZ13XFAETP. The ZTCs have total volumetric hydrogen uptake (at 20 bar and -196 $^oC$) of 24 and 46 g $l^{-1}$ for CZ13XFAET and CZ13XFAETP, respectively. Thus the total volumetric hydrogen uptake (at 20 bar) of the powdered ZTC is nearly doubled from 24 g $l^{-1}$ to 46 g $l^{-1}$ by performing the templating process with compacted zeolite pellets as template. Such a volumetric hydrogen uptake, at the relatively low pressure of 20 bar, is amongst the highest ever reported for any porous material, including densified carbons and MOFs.[25,40,44-50,54,61-68]

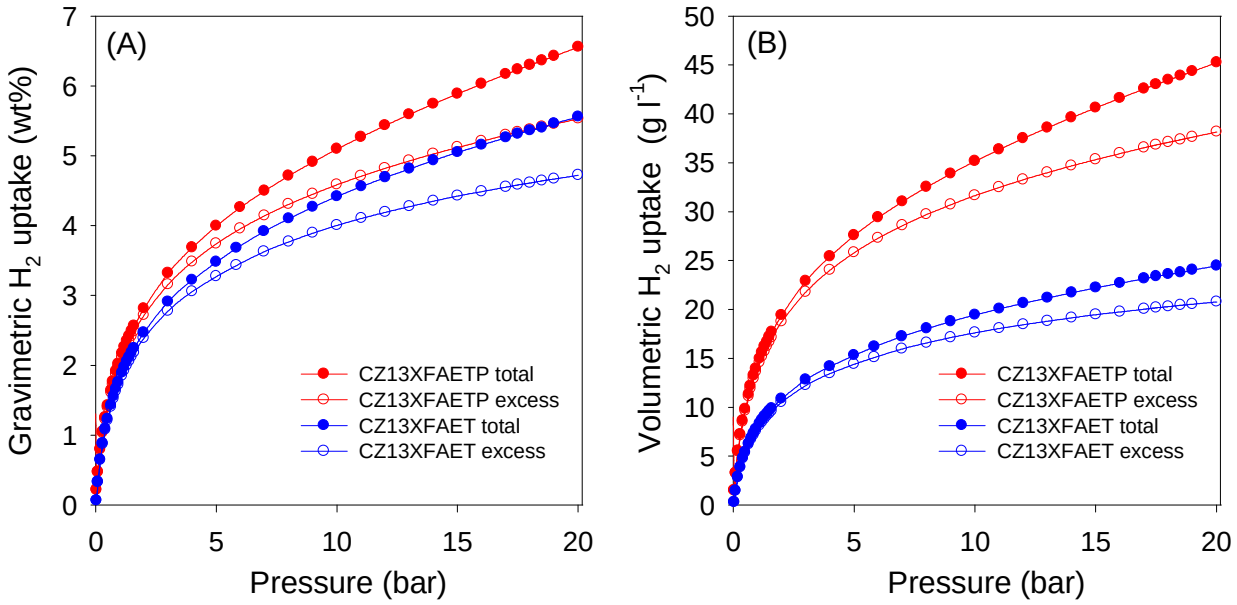


**Figure 10**. Gravimetric (A) and volumetric (B) excess and total hydrogen uptake isotherms at -196 $^{o}$C of zeolite templated carbons templated by powder (CZ13XFAET) or compacted pellets (CZ13XFAETP) of zeolite 13X.

The $CO_2$ uptake isotherms, obtained at 25 $^{o}$C, for the ZTCs prepared via the CVD + LI route are shown in Figure 11 and the storage capacity at 1 bar and 20 bar is given in Table 2. The gravimetric uptake capacity at 25 $^{o}$C and 1 bar (Figure 11A) is similar for both the powder CZ13XFAET (2.5 mmol $g^{-1}$) and pelletized CZ13XFAETP (2.6 mmol $g^{-1}$) samples. This is simply a reflection of the fact that low pressure $CO_2$ uptake is dependent on pore size and level of microporosity, variables that are similar for the two samples (Table 2). The higher surface area of the pelletized ZTC is reflected by the greater $CO_2$ uptake capacity at 20 bar of 22 mmol $g^{-1}$ compared to 18.6 mmol $g^{-1}$ for the powder sample, which is an increase of ca. 20%. More importantly, as shown in Figure 11B, the volumetric $CO_2$ uptake of the pelletized sample is far superior due to higher packing density. For example at 1 bar, CZ13XFAETP has an uptake of 79 g $l^{-1}$, which is 65% higher than that of CZ13XFAET (48 g $l^{-1}$). The superior volumetric uptake capacity of the pelletized sample increases at higher pressure such that at 20 bar it is nearly twice that of the

powdered sample; 668 g $l^{-1}$ compared to 360 g $l^{-1}$. A similar trend is observed for $CO_2$ uptake at 0 °C with slightly higher gravimetric uptake for the pelletized sample but much higher volumetric capacity (Table S2 and Supporting Figure S12).

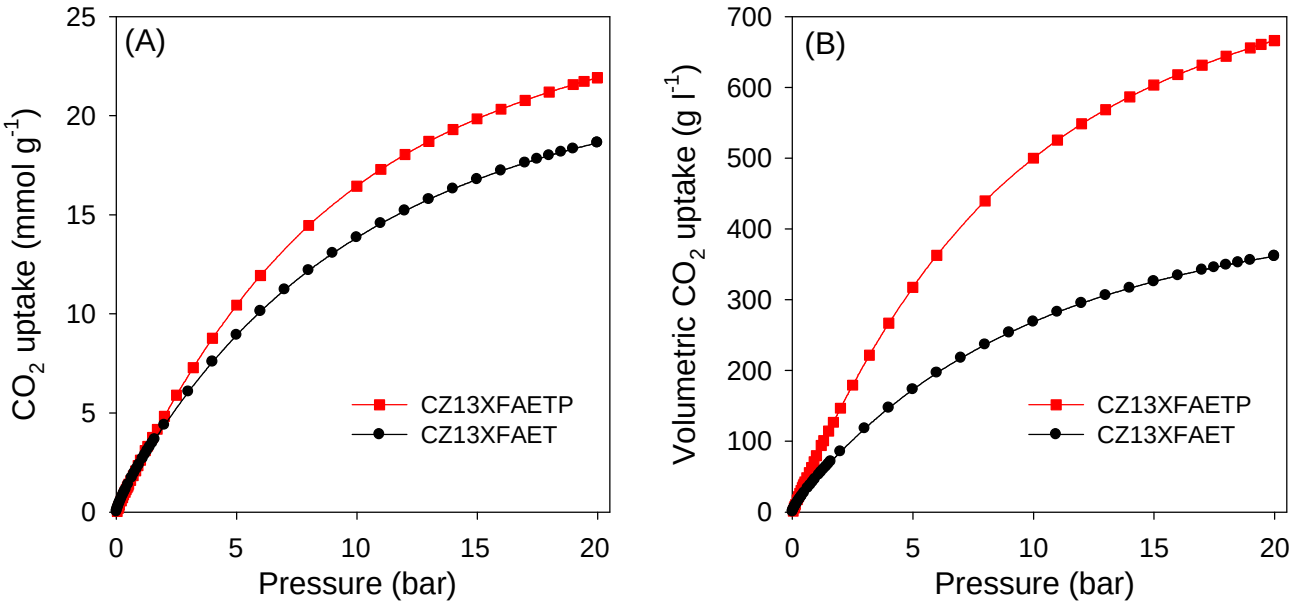


**Figure 9**. Gravimetric (A) and volumetric (B) $CO_2$ uptake at 25 °C and 0 - 20 bar for zeolite templated carbons templated by powder (CZ13XFAET) or compacted pellets (CZ13XFAETP) of zeolite 13X.

Templating of high surface area ZTCs with compacted zeolites therefore offers advantages with respect to the gravimetric and volumetric uptake of $CO_2$. Another critical measure of $CO_2$ uptake capacity is the so-called working capacity, which is especially relevant for pressure swing adsorption (PSA) processes that enable regeneration of the storage material. Comparing the $CO_2$ uptake at 20 bar (charging pressure) and atmospheric pressure (discharge/material regeneration pressure), the working capacity of the ZTCs is 19.4 and 16.1 mmol $CO_2$ $g^{-1}$ for CZ13XFAETP and CZ13XFAET, respectively. The gravimetric working capacity of 19.4 mmol $g^{-1}$ for the pelletized sample is comparable to the best adsorbents reported so far (Table S3). However, when the packing

density of the adsorbents is taken into account to calculate the volumetric uptake, the pelletized ZTC sample outperforms all currently available benchmark materials (Table S3). The volumetric working capacity of CZ13XFAETP is 589 g $l^{-1}$ (or 300 $cm^3$ $cm^{-3}$), which is higher than that of the best previously reported value of 529 g $l^{-1}$ (269 $cm^3$ $cm^{-3}$) for mesophase pitch-derived activated carbon.

## 4. Conclusions

A nanocasting process that utilizes compacted zeolite pellets as hard templates has been employed to generate pelletized zeolite template carbons (ZTCs) with moderate to high surface area and pore volume. The use of compacted zeolite pellets (following compression of powder forms of zeolites at 370 MPa or 740 MPa) rather than powdered forms of zeolites generates pelletized ZTCs with higher porosity and higher packing density. The rise in porosity and packing density does not, however, affect the pore size and pore size distribution. The higher porosity and packing density for the pelletized ZTCs translates to highly enhanced volumetric gas ($CO_2$ and hydrogen) uptake. For CVD-derived samples that exhibit moderate porosity, the pelletized ZTCs have surface area of ca. 2000 $m^2$ $g^{-1}$, which is 10% higher than for powder samples, despite an increase in packing density from ca. 0.55 to 0.85 g $cm^{-3}$. This means that the surface area per unit volume rises by ca. 60% from between 1000 and 1100 $m^2$ $cm^{-3}$ for the powder ZTCs to 1670 $m^2$ $cm^{-3}$ for pelletized samples. For the CVD-derived samples, the volumetric $CO_2$ uptake at 25 $^oC$ increases by 140% and 85% at 1 and 20 bar, respectively, to reach 101 g $l^{-1}$ (at 1 bar) and 531 g $l^{-1}$ (at 20 bar). Pelletized ZTCs prepared via a combination of liquid impregnation and CVD achieve much higher surface area above 3000 $m^2$ $g^{-1}$ (compared to 2700 $m^2$ $g^{-1}$ for powder samples). The increase in surface area occurs despite a simultaneous rise in packing density from 0.44 to 0.69 g $cm^{-3}$. The overall effect of this is that the surface area per unit volume rises by 75% from 1189 $m^2$ $cm^{-3}$ to 2085 $m^2$ $cm^{-3}$ for the pelletized sample. The high surface area pelletized ZTCs have attractive gravimetric hydrogen uptake of 6.6

wt% (5.5 wt% for powder sample) at 20 bar and -196 $^{o}$C, and due to their higher packing density have exceptional volumetric hydrogen storage capacity of 46 g $l^{-1}$ (24 g $l^{-1}$ for powder sample). For $CO_2$ uptake (at 25 $^{o}$C and 20 bar), the volumetric uptake of the high surface area pelletized ZTC is close to double that of the analogous powder sample, i.e., 668 g $l^{-1}$ compared to 360 g $l^{-1}$. In all cases the pelletized carbon samples also have higher gravimetric and volumetric gas uptake compared to directly compacted conventionally templated (with powdered zeolites) ZTCs. This study, and the findings herein described, present an entirely new route to microporous templated carbons and also break new ground with respect to levels of volumetric hydrogen uptake achievable for templated porous carbons. The findings add new insights in the development of carbonaceous materials with enhanced properties for the storage of energy related gases. The pelletized ZTCs may also be used for storage of other gases such as methane, acetylene and natural gas.

## Acknowledgements

The assistance of Dr Elizabeth Steer (SEM images) and Dr Graham Rance (Raman spectra) at the Nottingham Nanoscale and Microscale Research Centre (nmRC) is gratefully acknowledged. We thank the government of the Kingdom of Saudi Arabia for funding a PhD studentship for NB.

## Supporting Information

Three Tables with textural data, $CO_2$ uptake at 0 $^{o}$C and benchmarking data, and twelve additional figures showing; SEM images, XRD patterns, Raman spectra, nitrogen sorption isotherms, pore size distribution curves, TGA curves and $CO_2$ uptake isotherms at 0 $^{o}$C.

## References


1. L. Schlapbach and A. Züttel, *Nature* 2001, **414**, 353.

2. J. A. Turner, *Science* 1999, **285**, 687.

3. L. L. Zhang and X. S. Zhao, *Chem. Soc. Rev.*, 2009, **38** 2520.

4. M. Sevilla and R. Mokaya, *Energy Environ. Sci*., 2014, **7**, 1250.

5. L. Wei and G. Yushin, *Nano Energy*, 2012, **1,** 552.

6. S. Choi, J. H. Drese and C. W. Jones, *ChemSusChem*, 2009, **2**, 796.

7. Q. Wang, J. Luo, Z. Zhong and A. Borgna, *Energy Environ. Sci*., 2011, **4**, 42.

8. D. M. D'Alessandro, B. Smit and J. R. Long, *Angew. Chem. Int. Ed*., 2010, **49**, 6058.

9. S. Wang, S. Yan, X. Ma and J. Gong, *Energy Environ. Sci*., 2011, **4**, 3805.

10. K. Sumida, D. L. Rogow, J. A. Mason, T. M. McDonald, E. D. Bloch, Z. R. Herm, T.-H. Bae and J. R. Long, *Chem. Rev*., 2012, **112**, 724.

11. H. Furukawa, N. Ko, Y. B. Go, N. Aratani, S. B. Choi, E. Choi, A. O. Yazaydin, R. Q. Snurr, M. O'Keeffe, J. Kim and O. M. Yaghi, *Science*, 2010, **329**, 424.

12. A. O. Yazaydin, A. I. Benin, S. A. Faheem, P. Jakubczak, J. J. Low, R. R. Willis and R. Q. Snurr, *Chem. Mater.*, 2009, **21**, 1425.

13. M. Sevilla and A. B. Fuertes, *Energy Environ. Sci*., 2011, **4**, 1765.

14. M. Sevilla, P. Valle-Vigon and A. B. Fuertes, *Adv. Funct. Mater.*, 2011, **21**, 2781.

15. V. Presser, J. McDonough, S.-H. Yeon and Y. Gogotsi, *Energy Environ. Sci*., 2011, **4**, 3059.

16. J. Silvestre-Albero, A. Wahby, A. Sepulveda-Escribano, M. Martinez-Escandell, K. Kaneko and F. Rodriguez-Reinoso, *Chem. Commun*., 2011, **47**, 6840.

17. E. Masika and R. Mokaya, *RSC Adv.*, 2013, **3**, 17677.

18. Y. D. Xia, R. Mokaya, G. S. Walker and Y. Q. Zhu, *Adv. Energy Mater.*, 2011, **1**, 678.

19. M. Sevilla, A. B. Fuertes and R. Mokaya R. *Energy Environ. Sci*., 2011, **3**, 1400.

20. A. W. C. van den Berg and C. O. Arean, *Chem. Commun.*, 2008, 668.

21. H. Furukawa, K. E. Cordova, M. O'Keeffe and O. M. Yaghi, *Science*, 2013, **341**, 974.

22. Y. H. Xu, S. B. Jin, H. Xu, A. Nagai and D. L. Jiang, *Chem. Soc. Rev.*, 2013, **42** 8012.

23. Y. Xia, Z. Yang and R. Mokaya, *Nanoscale*, 2010, **2**, 639.

24. H. Nishihara and T. Kyotani, *Adv. Mater.*, 2012, **24**, 4473.

25 A. Almasoudi and R. Mokaya, *J. Mater. Chem. A*, 2014, **2**, 10960.

26. Y. X. Xia, Z. X. Yang and Y. Zhu, *J. Mater. Chem. A*, 2013, **1** 9365.

27. J. C. Wang and S. Kaskel, *J. Mater. Chem*., 2012, **22**, 23710.

28. T. Kyotani, T. Nagai, S. Inoue and A. Tomita, *Chem. Mater.*, 1997, **9**, 609.

29. Z. Yang, Y. Xia and R. Mokaya, *J. Am. Chem. Soc.*, 2007, **129**, 1673.

30. Y. Xia, G. S. Walker, D. M. Grant and R. Mokaya, *J. Am. Chem. Soc.*, 2009, **131**, 16493.

31. Y. Xia, R. Mokaya, D. M. Grant and G. S. Walker, *Carbon*, 2011, **49**, 844.

32. U.S. Department of Energy Website: https://www1.eere.energy.gov /hydrogenandfuelcells/storage/current_technology.html.

33. B. Adeniran and R. Mokaya, *Chem. Mater.* 2016, **28**, 994.

34. M. Sevilla J. B. Parra and A. B. Fuertes, *ACS Appl. Mater. Interfaces*, 2013, **5**, 6360.

35. B. Adeniran and R. Mokaya, *J. Mater. Chem. A*, 2015, **3**, 5148.

36. K. V. Kumar, K. Preuss, L. Lu, Z. X. Guo and M. M. Titirici, *J. Phys. Chem. C*, 2015, **119**, 22310.

37. B. Adeniran, E. Masika and R. Mokaya, *J. Mater. Chem. A*, 2014, **2**, 14696.

38. H. M. Coromina, D. A. Walsh and R. Mokaya, R. *J. Mater. Chem. A* 2016, 4, 280.

39. W. Sangchoom and R. Mokaya, *ACS Sust. Chem. Eng*., 2015, **3**, 1658

40. J. P. Marco-Lozar, J. Juan-Juan, F. Suarez-Garcıa, D. Cazorla-Amoros and A. Linares-Solano, *Int. J. Hydrogen Energy*, 2012, **37**, 2370.

41. J. Juan-Juan, J. P. Marco-Lozar, F. Suarez-Garcia, D. Cazorla-Amoros and A. Linares-Solano, *Carbon*, 2010, **48**, 2906.

42. K. W. Chapman, G. J. Halder and P. J. Chupas, *J. Am. Chem. Soc*., 2009, **131**, 17546.

43. J. Alcaniz-Monge, G. Trautwein, M. Perez-Cadenas and M. C. Roman-Martinez, *Microporous Mesoporous Mater*., 2009, **126**, 291.

44. M. Jorda-Beneyto, D. Lozano-Castello, F. Suarez-Garcıa, D.Cazorla-Amoros and A. Linares-Solano, *Microporous Mesoporous Mater*., 2008, **112**, 235.

45. L. Zhou, Y. Zhou and Y. Sun, *Int. J. Hydrogen Energy*, **2004**, *29*, 319.

46. B. Adeniran and R. Mokaya, *Nano Energy*, 2015, **16**, 173.

47. U. Mueller, M. Schubert, F. Teich, H. Puetter, K. Schierle-Arndt and J. Pastre, *J. Mater. Chem*., 2006, **16**, 626.

48. R. Zacharia, D. Cossement, L. Lafi and R. Chahine, *J. Mater. Chem*., 2010, **20**, 2145.

49. J. J. Purewal, D. Liu, J. Yang, A. Sudik, D. J. Siegel, S. Maurer and U. Muller *Int. J. Hydrogen Energy* 2012, **37**, 2723.

50. J. Purewal, D. Liu, A. Sudik, M. Veenstra, J. Yang, S. Maurer, U. Muller, and D. J. Siegel *J. Phys. Chem. C,* 2012, **116**, 20199.

51. J. P. Marco-Lozar, M. Kunowsky, F. Suarez-Garcia, J. D. Carruthers and A. Linares-Solano, *Energy Environ. Sci*., 2012, **5**, 9833.

52. N. Balahmar, A. C. Mitchell, and R. Mokaya, *Adv. Energy Mater.*, **2015**, *5*, 1500867.

53. P. X. Hou, H. Orikasa, H. Itoi, H. Nishihara and T. Kyotani, *Carbon*, 2007, **45**, 2011.

54. E. Masika and R. Mokaya, *Energy Environ. Sci*., 2014, **7**, 427.

55. Z. X. Yang, Y. D. Xia, X. Z. Sun and R. Mokaya, *J. Phys. Chem. B*, 2006, **110**, 18424.

56. C. Portet, Z. Yang, Y. Korenblit, Y. Gogotsi, R. Mokaya and G. Yushin, *J. Electrochem. Soc.*, 2009, **156**, A1-A6.

57. H. Nishihara, Q. H. Yang, P. X. Hou, M. Unno, S. Yamauchi, R. Saito, J. I. Paredes, A. Martínez-Alonso, J. M.D. Tascón, Y. Sato, M. Terauchi and T. Kyotani, *Carbon*, **2009**, 47, 1220.

58. N. Alam and R. Mokaya, *Energy Environ. Sci.*, 2010, **3**, 1773.

59. T. Kyotani, Z. Ma and A. Tomita, *Carbon*, 2003, **41**, 1451.

60. F. O. M. Gaslain, J. Parmentier, V. P. Valtchev and J. Patarin, *Chem. Commun.*, 2006, 991.

61. M. Sevilla, R. Mokaya and A. B. Fuertes, *Energy Environ. Sci.*, 2011, **4**, 2930.

62. H. Nishihara, P. X. Li, L. X. Hou, M. Ito, M. Uchiyama, T. Kaburagi, A. Ikura, J. Katamura, T. Kawarada, K. Mizuuchi and T. Kyotani, *J. Phys. Chem. C*, 2009, **113**, 3189.

63. N. P. Stadie, J. J. Vajo, R. W. Cumberland, A. A. Wilson, C. C. Ahn, and B. Fultz, *Langmuir* 2012, **28**, 10057.

64. S. S. Kaye, A. Dailly, O. M. Yaghi and J. R. Long, *J. Am. Chem. Soc*., 2007, **129**, 14176.

65. Y. Peng, V. Krungleviciute, I. Eryazici, J. T. Hupp, O. K. Farha and T. Yildirim, *J. Am. Chem. Soc*., 2013, **135**, 11887. H. Furukawa, M. A. Miller and O. M. Yaghi, *J. Mater. Chem.* 2007, **17**, 3197.

66. Y. Yan, X. Lin, S. Yang, A. J. Blake, A. Dailly, N. R. Champness, P. Hubberstey and M. Schroder, *Chem. Commun*. 2009, 1025.

67. O. K. Farha, A. O. Yazaydın, I. Eryazici, C. D. Malliakas, B. G. Hauser, M. G. Kanatzidis, S. T. Nguyen, R. Q. Snurr and J. T. Hupp, *Nat. Chem*. 2010, **2**, 944.

68. A. Dailly and E. Poirier, *Energy Environ. Sci*. 2011, **4**, 3527.

## Graphical Abstract

Zeolite pellets compacted at 370 to 740 MPa may be used as hard templates for the nanocasting of pelletized zeolite templated carbons (ZTCs) with simultaneously enhanced porosity (up to 3000 $m^2$ $g^{-1}$) and high packing density (0.69 – 0.88 g $cm^{-3}$); the pelletized ZTCs have excellent volumetric gas storage capacity of 46 g $l^{-1}$ of hydrogen at 20 bar and -196 $^oC$ (compared to 24 g $l^{-1}$ for powdered ZTC), and $CO_2$ uptake of 668 g $l^{-1}$ at 25 $^oC$ and 20 bar (compared to 360 g $l^{-1}$ for powdered ZTC).

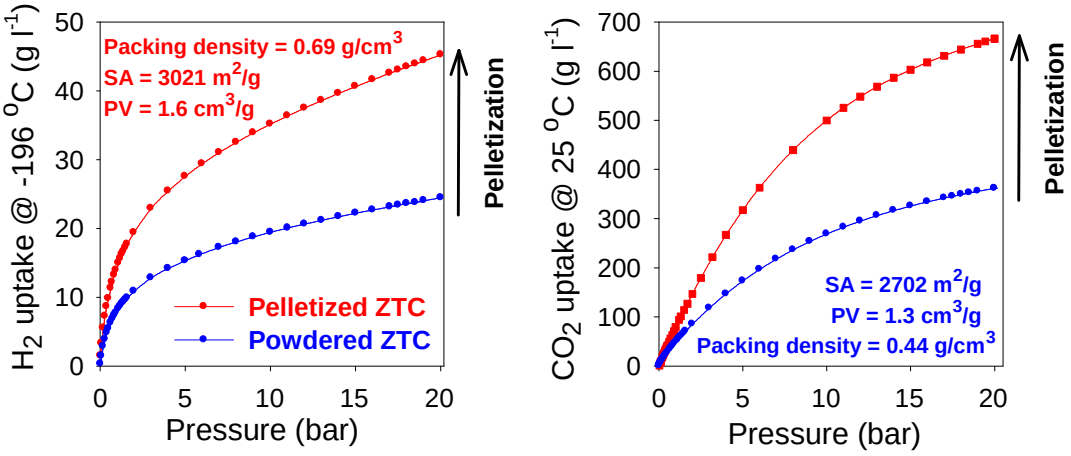

*Supporting Information*

# Templating of carbon in zeolites under pressure: Synthesis of pelletized zeolite templated carbons with improved porosity and packing density for superior gas ($CO_2$ and $H_2$) uptake properties

Norah Balahmar, Alexander M. Lowbridge and Robert Mokaya*

University of Nottingham, University Park, Nottingham NG7 2RD, U. K.

*E-mail: r.mokaya@nottingham.ac.uk (R. Mokaya)*

**Table S1**. Textural properties of zeolite 13X before and after compaction at 740 MPa

| Sample | Surface area[a] ($m^2$ $g^{-1}$) | Pore volume[b] ($cm^3$ $g^{-1}$) | Pore size[c] (Å) |
|---|---|---|---|
| Z13X | 717 (705) | 0.33 (0.31) | 7.5/10 |
| Z13X@740MPa | 692 (680) | 0.32 (0.30) | 7.5/10 |

The values in the parenthesis refer to: [a]micropore surface area and [b]micropore volume. [c]pore size distribution maxima obtained from NLDFT analysis.

**Table S2**. $CO_2$ uptake at 0 $^oC$ for zeolite templated carbons templated by powder (CZ13XFAET) or compacted pellets (CZ13XFAETP) of zeolite 13X.

| Sample | $CO_2$ uptake[a] (mmol/g) | | Working capacity[b] (mmol/g) |
|---|---|---|---|
| | 1 bar | 20 bar | |
| CZ13XFAET | 4.3 (83) | 23.2 (449) | 18.9 (366) |
| CZ13XFAETP | 4.5 (137) | 26.0 (789) | 21.5 (652) |

The values in the parenthesis are volumetric $CO_2$ uptake in g $l^{-1}$. [a]$CO_2$ uptake at 25 $^oC$ and various pressures (i.e., 1 bar and 20 bar). [b]Defined as the difference of storage capacity between 20 and 1 bar.

**Table S3.** $CO_2$ uptake at 25 ºC and 20 bar, and working capacity for PSA (20 bar to 1 bar) for powder (CZ13XFAET) and pelletized (CZ13XFAETP) ZTCs compared to top-performing materials reported in the literature.

| Material | Packing density ($g/cm^3$) | $CO_2$ uptake (20 bar, 25 ºC) (mmol/g) | Working capacity for PSA system[a] | | | Reference |
|---|---|---|---|---|---|---|
| | | | (mmol/g) | (g/l) | ($cm^3/cm^3$) | |
| CZ13XFAETP | 0.69 | 22.0 | 19.4 | 589 | 300 | This work |
| CZ13XFAET | 0.44 | 18.6 | 16.1 | 312 | 159 | This work |
| VR-5 (AC from mesophase pitch) | 0.47 | 26.8 | 22.0 | 455 | 232 | 1 |
| VR-93 (AC from mesophase pitch) | 0.47 | 30.4 | 25.6 | 529 | 269 | 1 |
| VR5-4:1 (AC from mesophase pitch) | 0.47 | 22.0 | 19.4 | 401 | 204 | 2 |
| Maxsorb (comercial AC) | 0.29 | 19.0 | 16.9 | 216 | 110 | 3 |
| HPC5b2-1100 (hierarchical carbon) | | 20.8 | 17.1 | | | 4 |
| MOF-5 | 0.31[b] | 19.3 | 18.5 | 252 | 128 | 4,5,6 |
| MOF-177 | 0.21[c] | 28.1 | 27.1 | 250 | 127 | 7,8,9 |

[a]Defined as the difference of storage capacity between 20 and 1 bar. [b] Packing (or pellet) density according to ref 5 and 6. [c] Packing density according to ref 8 and 9.

## References


1. J. Silvestre-Albero, A. Wahby, A. Sepulveda-Escribano, M. Martinez-Escandell, K. Kaneko and F. Rodriguez-Reinoso, *Chem. Commun*., 2011, **47**, 6840.
2. M. E. Casco, M. Martínez-Escandell, J. Silvestre-Albero and F. Rodríguez-Reinoso, *Carbon* **2014**, *67*, 230-235.
3. S. Himeno, T. Komatsu and S. Fujita, *J. Chem. Eng. Data* **2005**, *50*, 369-376.
4. G. Srinivas, V. Krungleviciute, Z.-X. Guo and T. Yildirim, *Energy Environ. Sci.* **2014**, *7*, 335-342.
5. A. Dailly and E. Poirier, *Energy Environ. Sci*. 2011, **4**, 3527–3534.
6. R. Zacharia, D. Cossement, L. Lafi and R. Chahine, *J. Mater. Chem.* 2010, **20**, 2145–2151.
7. A. R. Millward and O. M. Yaghi, *J. Am. Chem. Soc.* **2005**, *127*, 17998-17999.
8. J. Purewal, D. Liu, A. Sudik, M. Veenstra, J. Yang, S. Maurer, U. Muller and D. J. Siegel, *J. Phys. Chem. C* **2012**, *116*, 20199−20212.
9. J. Purewal, D. Liu, J. Yang, A. Sudik, D. Siegel, S. Maurerand U. Mueller, *Int. J. Hydrogen Energy* **2012**, *37*, 2723−2727.

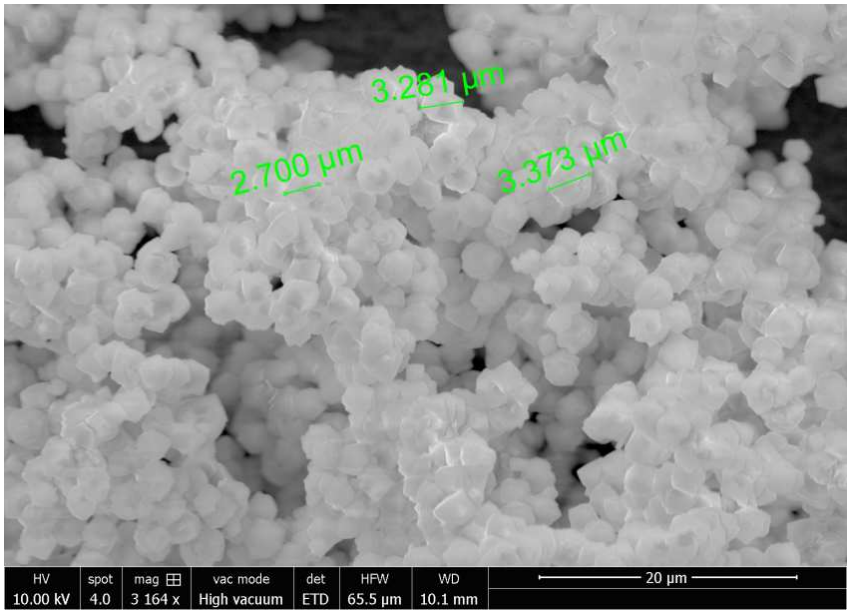


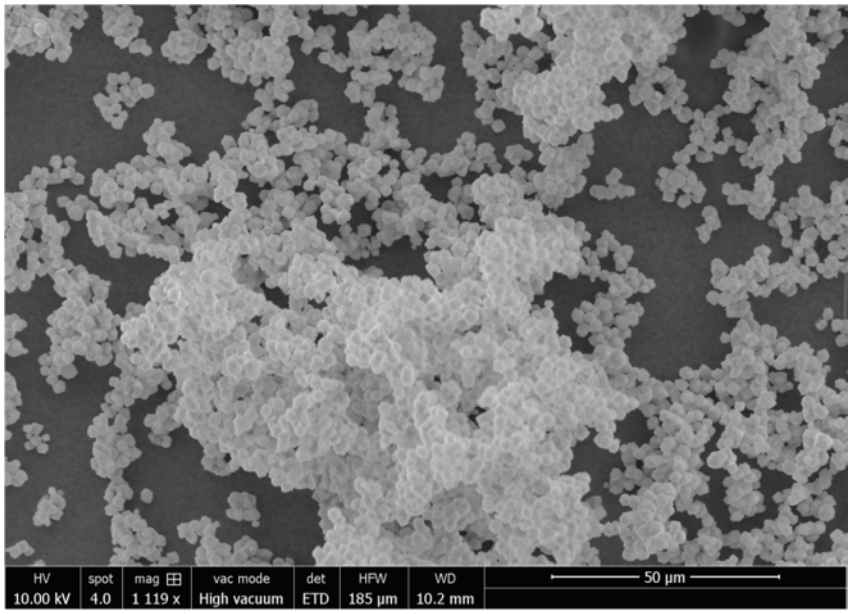


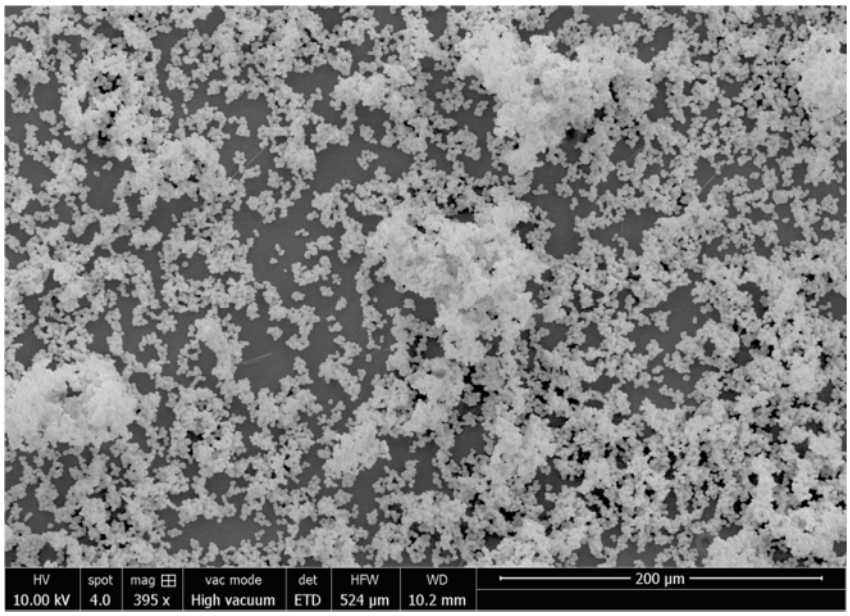


**Figure S1**. SEM images of powdered zeolite 13X

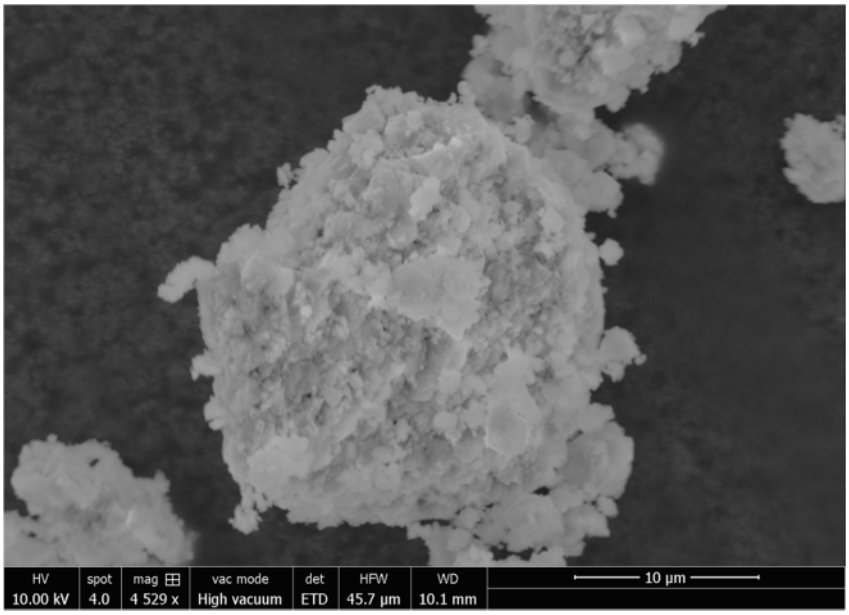


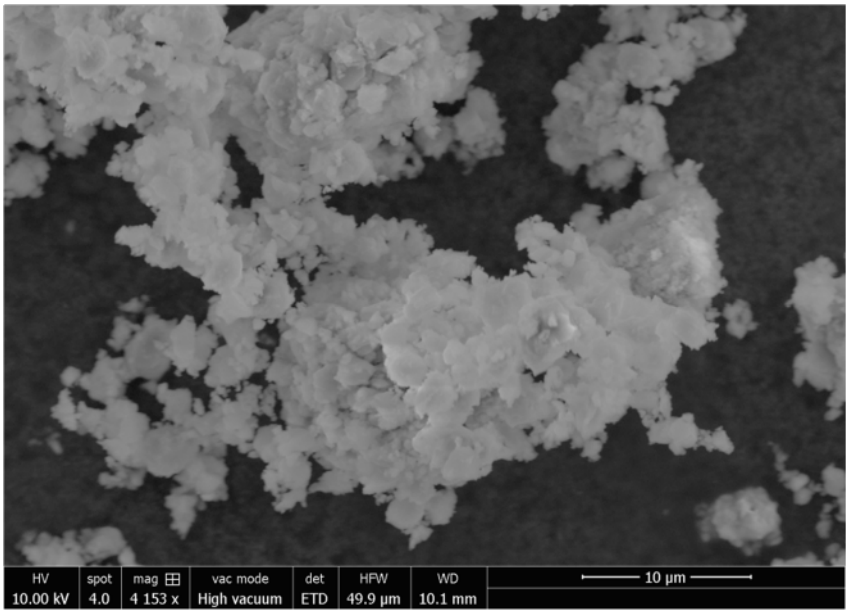


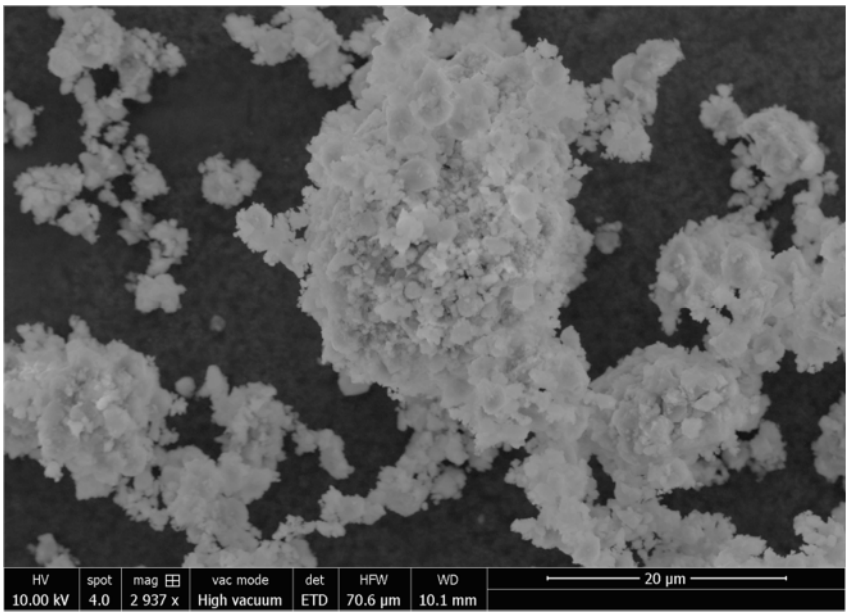


**Figure S2**. SEM images of zeolite 13X compacted at 5 tonnes (370 MPa)

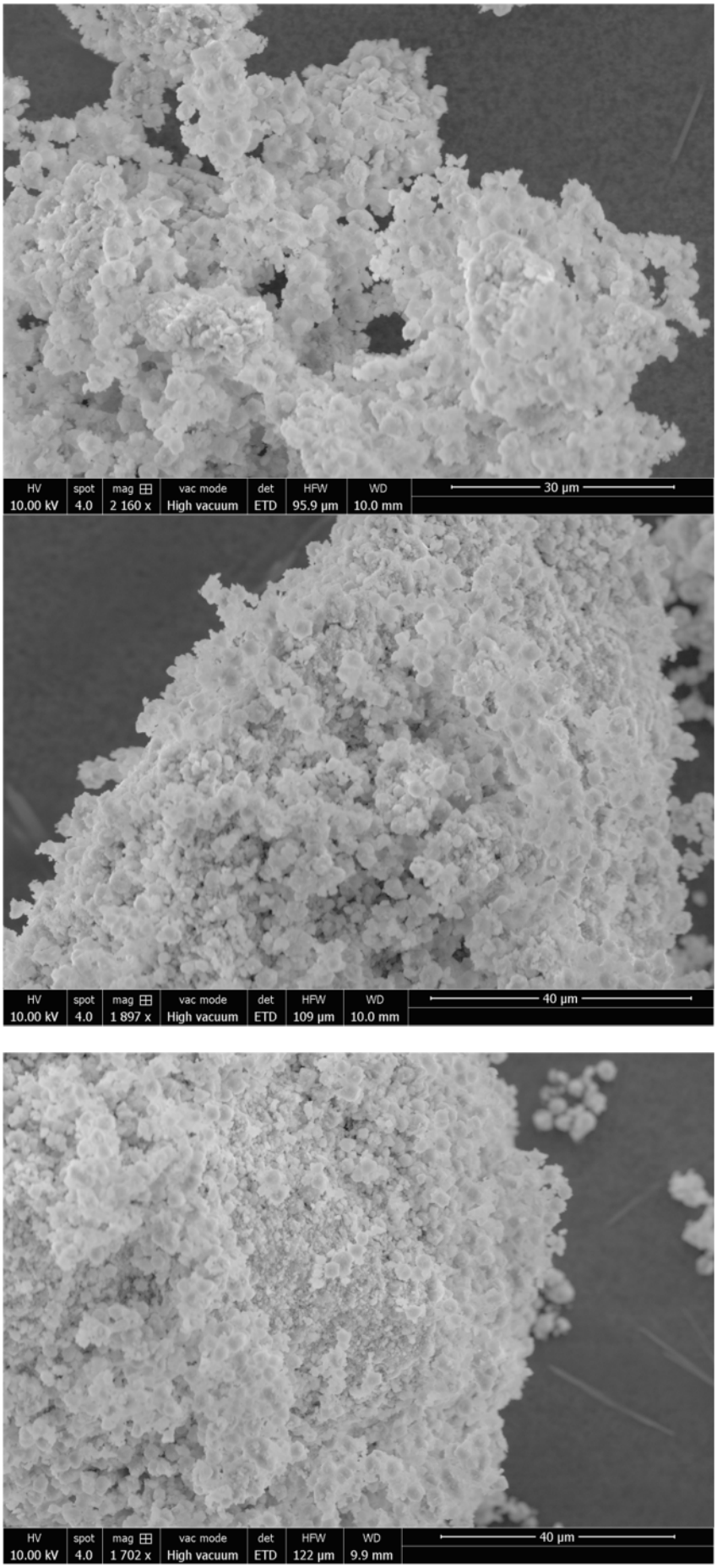


**Figure S3**. SEM images of zeolite 13X compacted at 10 tonnes (740 MPa)

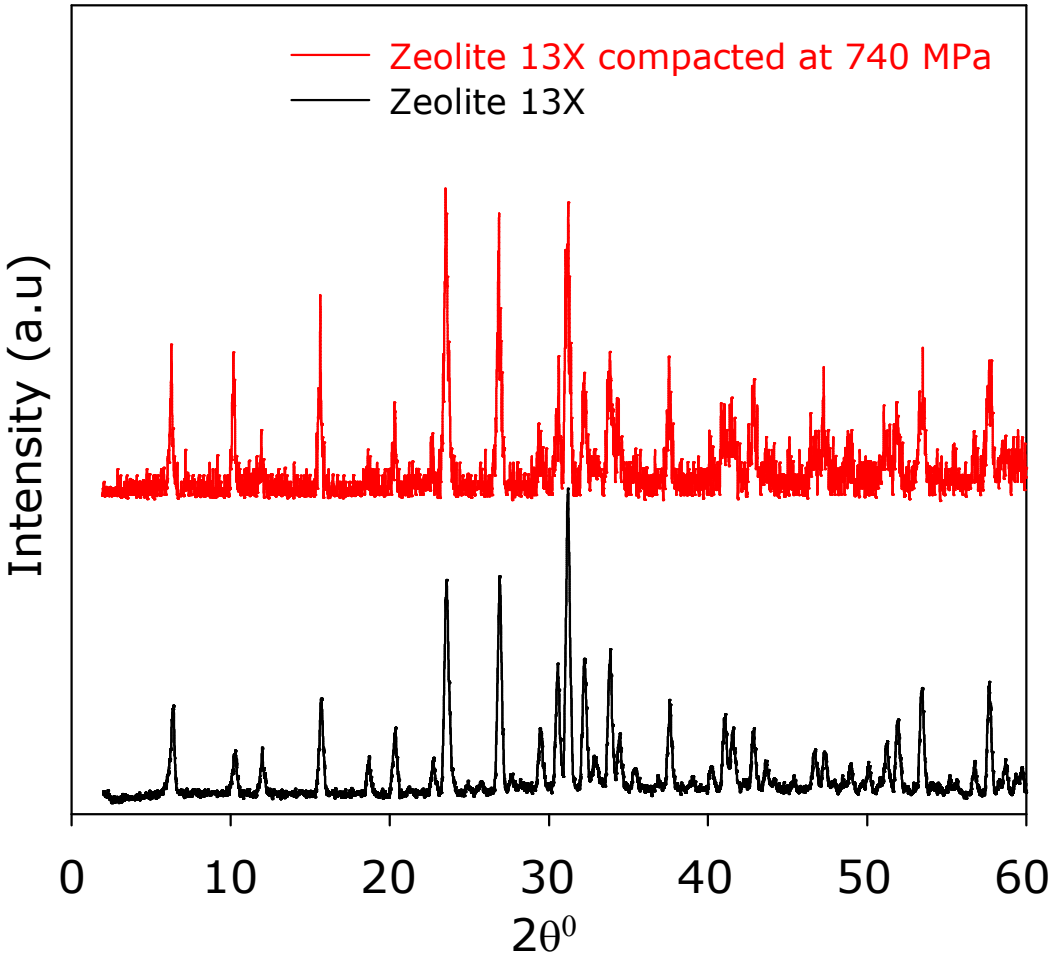


**Figure S4**. Powder XRD patterns of zeolite 13X before and after compaction and 740 MPa. The XRD patterns remain unchanged, which indicates that the structural ordering of the zeolite is preserved after compaction.

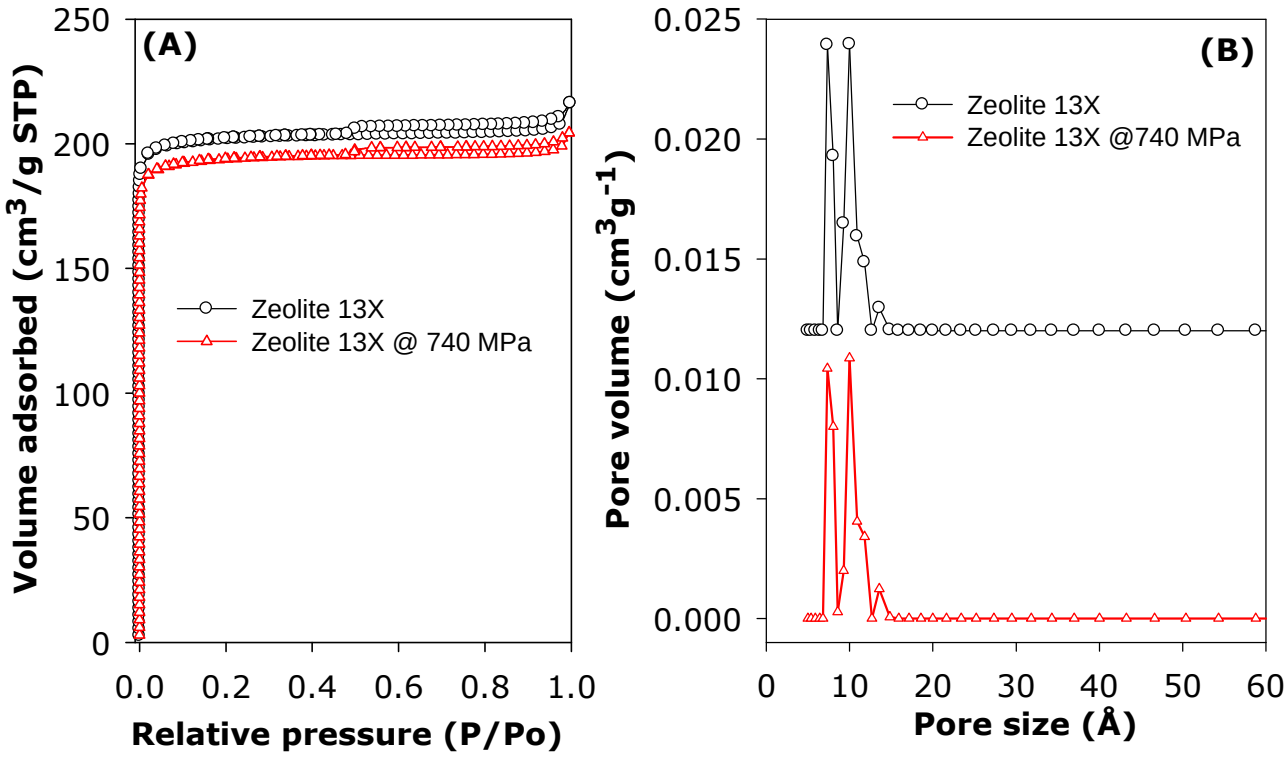


**Figure S5**. Nitrogen sorption isotherms (A) and corresponding pore size distribution (PSD) curves (B) of zeolite 13X before and after compaction at 740 MPa.

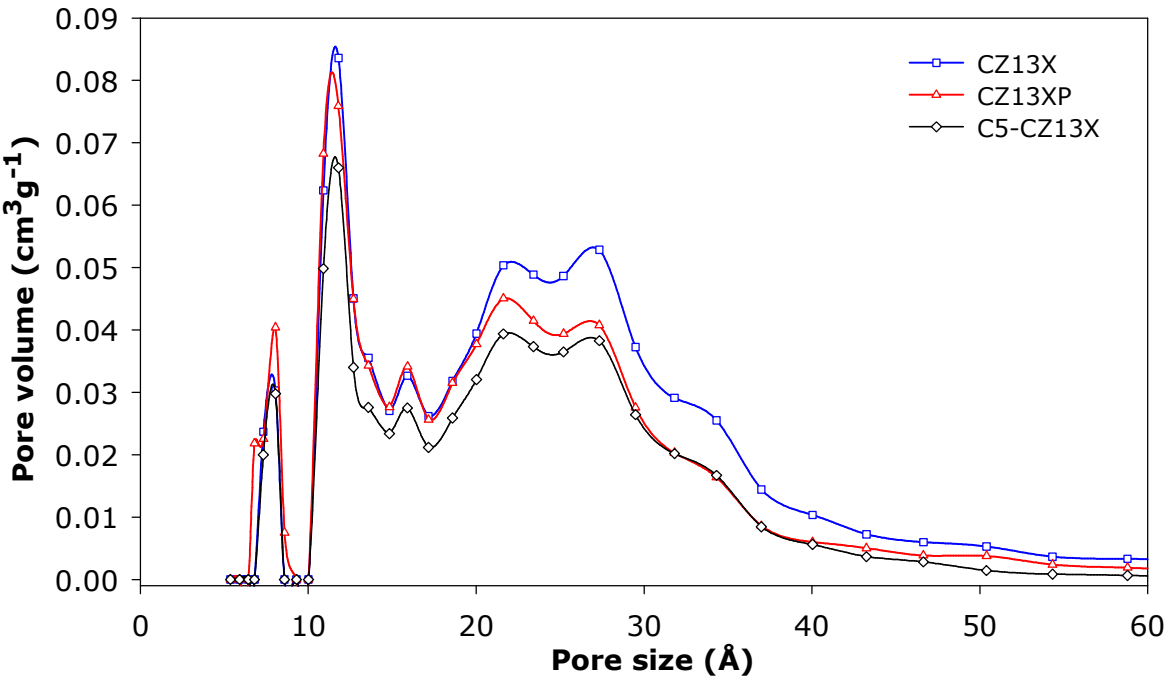


**Figure S6**. Pore size distribution curves of zeolite templated carbons prepared via a CVD route using powder (C13X) or compacted pellets (C13XP) of zeolite 13X as hard template. Sample C5-CZ13X is a directly compacted (at 370 MPa) form of CZ13X.

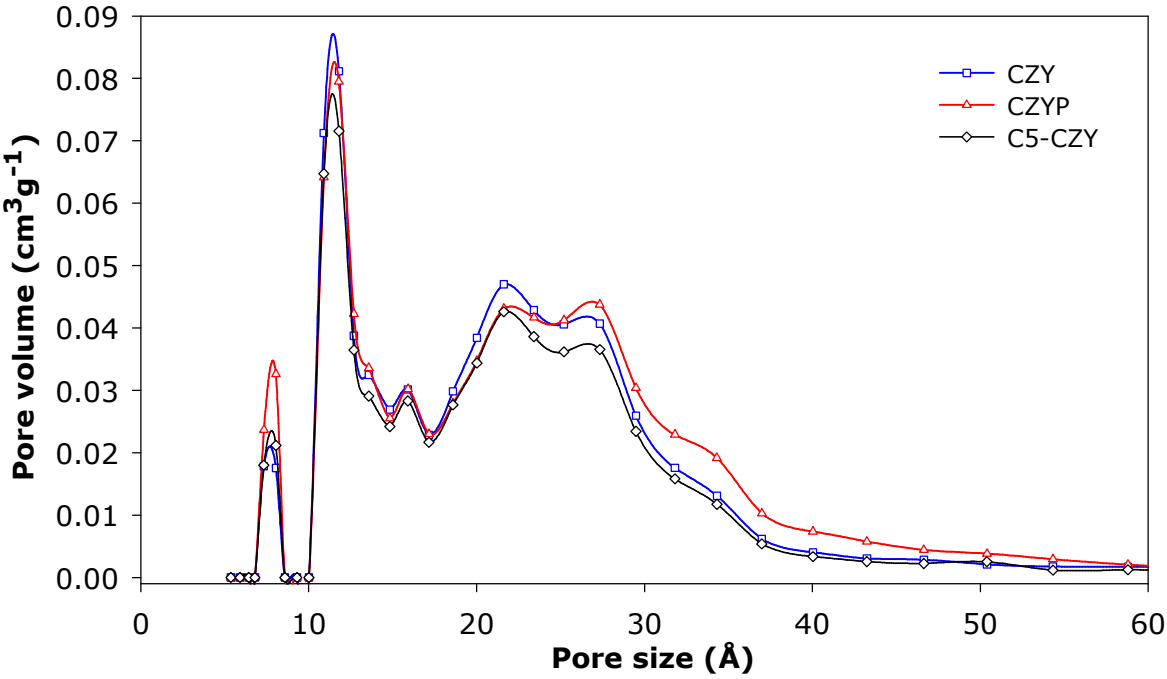


**Figure S7**. Pore size distribution curves of zeolite templated carbons prepared via a CVD route using powder (CZY) or compacted pellets (CZYP) of zeolite Y as hard template. Sample C5-CZY is a directly compacted (at 370 MPa) form of CZY.

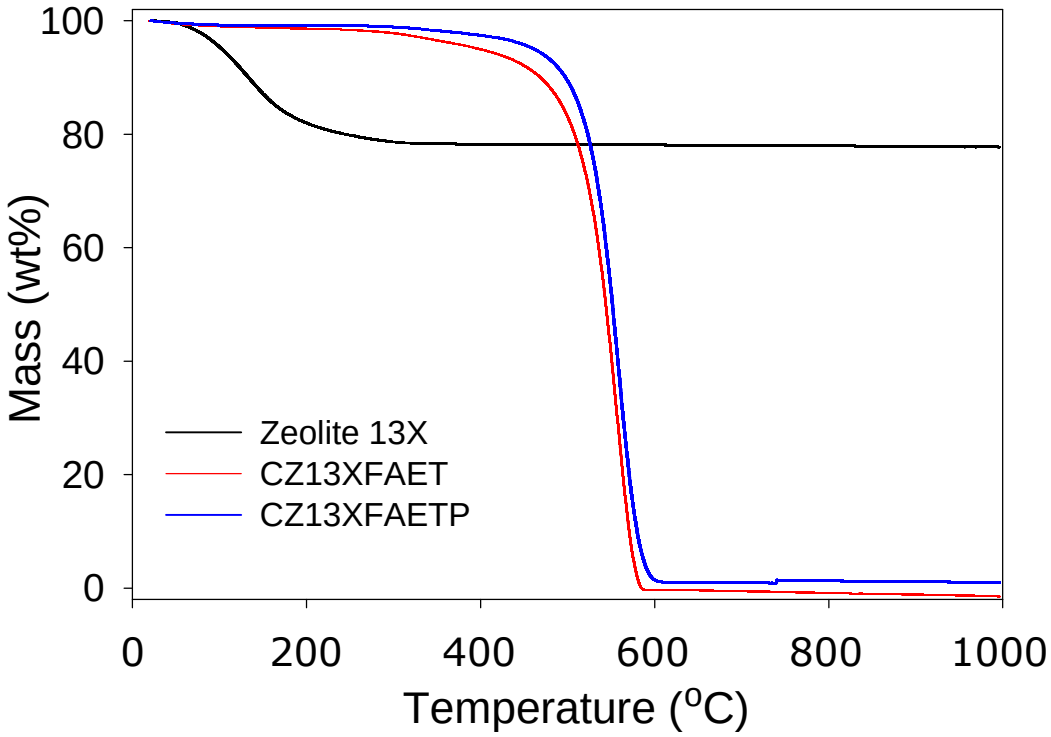


**Figure S8**. Thermogravimetric analysis (TGA) curves of zeolite 13X, and zeolite templated carbons prepared via a route that combines liquid impregnation and CVD using powder (CZ13XFAET) or compacted pellets (CZ13XFAETP) of zeolite 13X as hard template. The TGA was performed under flowing air conditions.

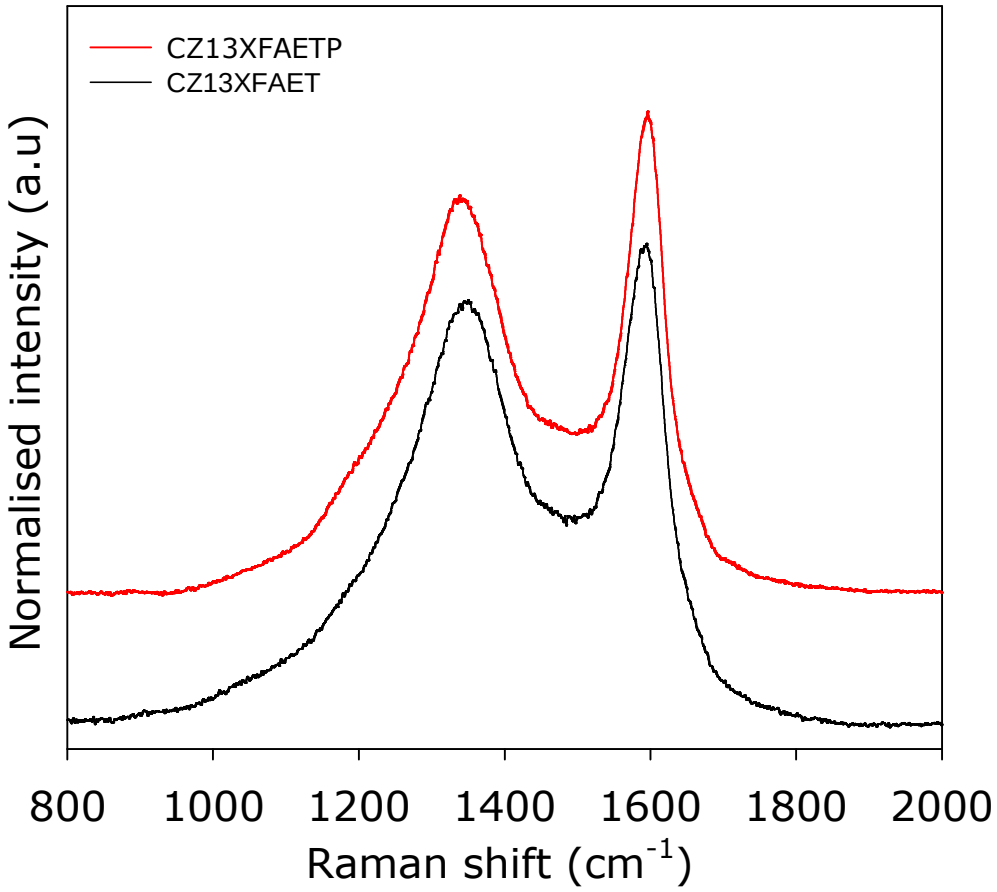


**Figure S9.** Raman spectra of zeolite templated carbons prepared via a route that combines liquid impregnation and CVD using powder (CZ13XFAET) or compacted pellets (CZ13XFAETP) of zeolite 13X as hard template.

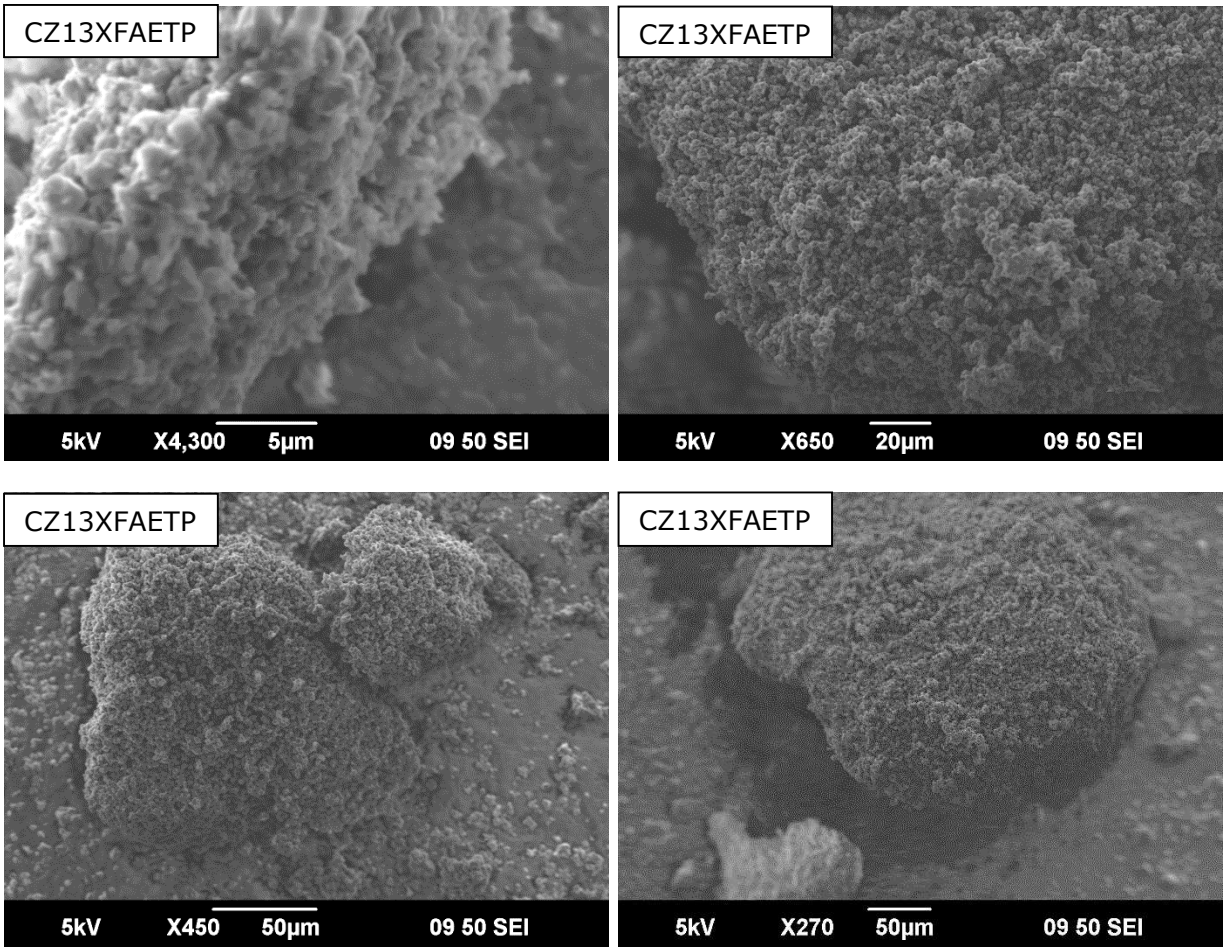


**Figure S10.** Raman spectra of zeolite templated carbons prepared via a route that combines liquid impregnation and CVD using powder (CZ13XFAET) or compacted pellets (CZ13XFAETP) of zeolite 13X as hard template.

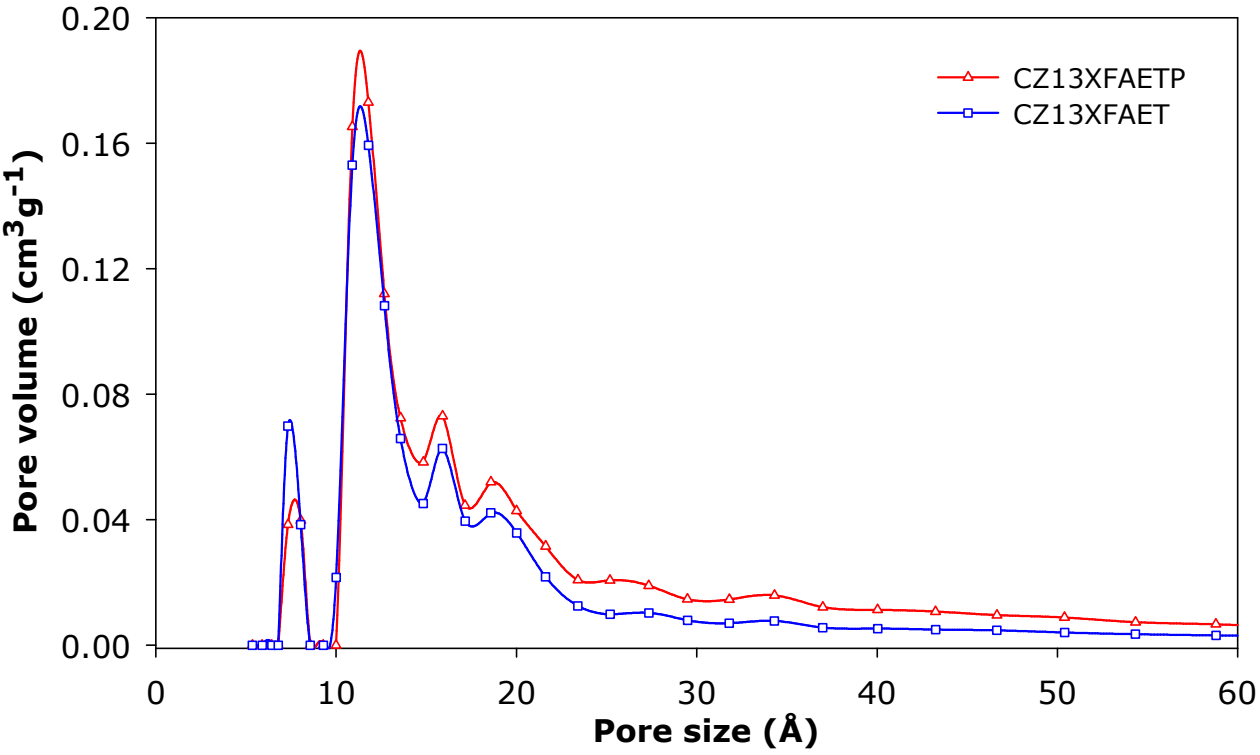


**Figure S11**. Pore size distribution curves of zeolite templated carbons prepared via a route that combines liquid impregnation and CVD using powder (CZ13XFAET) or compacted pellets (CZ13XFAETP) of zeolite 13X as hard template.

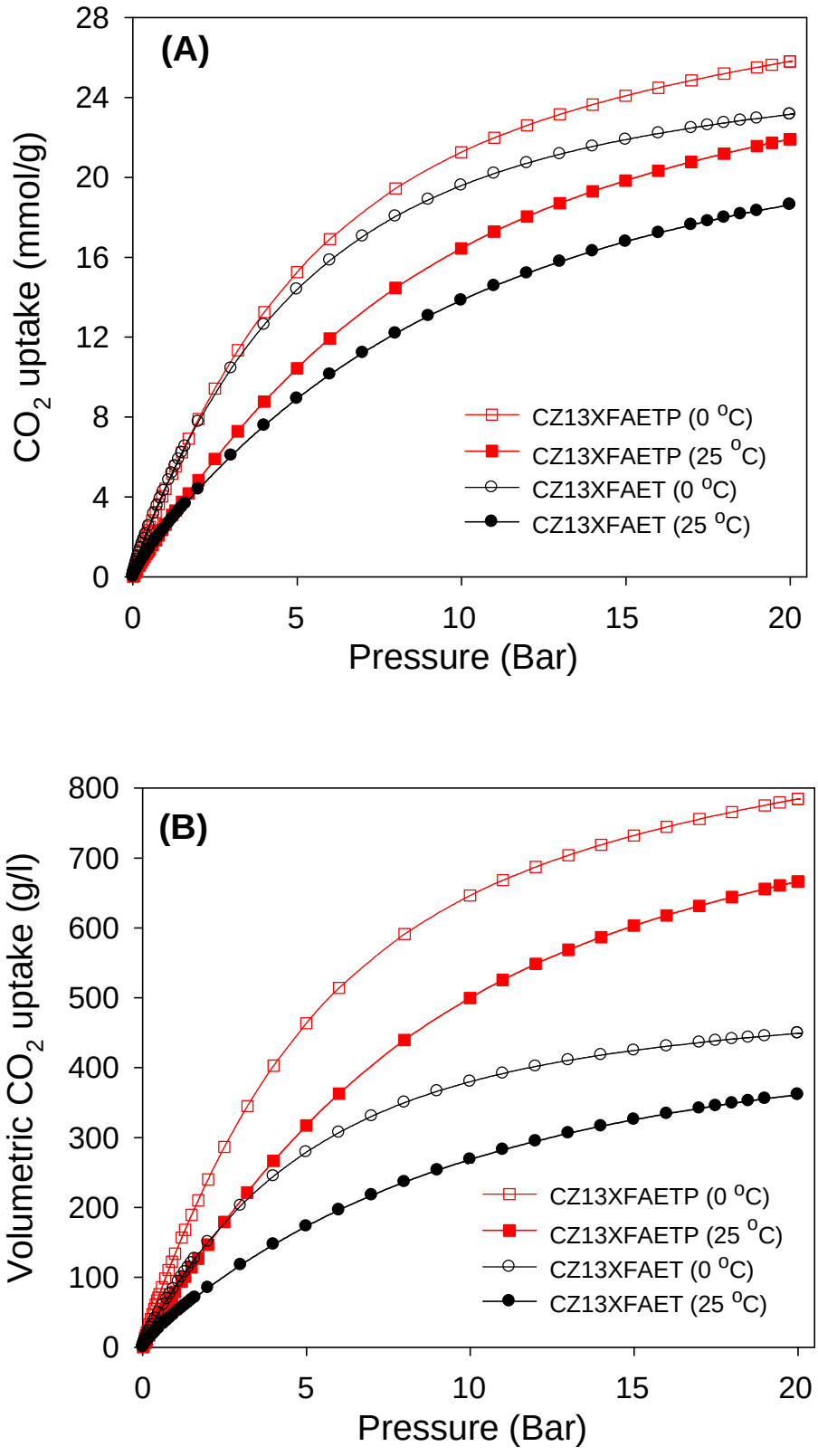


**Figure S12**. Gravimetric (A) and volumetric (B) $CO_2$ uptake at 0 °C or 25 °C and 0 - 20 bar for zeolite templated carbons templated by powder (CZ13XFAET) or compacted pellets (CZ13XFAETP) of zeolite 13X.